ISTANBUL TECHNICAL UNIVERSITY ★ GRADUATE SCHOOL OF SCIENCE ENGINEERING AND TECHNOLOGY

MOLECULAR DYNAMICS STUDY OF THE THERMAL CONDUCTIVITY IN NANOFLUIDS

M.Sc. THESIS

İrem TOPAL

Department of Physics Engineering

Physics Engineering Programme

AUGUST 2017

ISTANBUL TECHNICAL UNIVERSITY ★ GRADUATE SCHOOL OF SCIENCE ENGINEERING AND TECHNOLOGY

MOLECULAR DYNAMICS STUDY OF THE THERMAL CONDUCTIVITY IN NANOFLUIDS

M.Sc. THESIS

İrem TOPAL
(509141104)

Department of Physics Engineering

Physics Engineering Programme

Thesis Advisor: Assoc. Prof. Cem SERVANTIE

AUGUST 2017

İSTANBUL TEKNİK ÜNİVERSİTESİ ★ FEN BİLİMLERİ ENSTİTÜSÜ

NANOAKIŞKANLARDA TERMAL İLETKENLİĞİN MOLEKÜLER DİNAMİK HESAPLAMALARI

YÜKSEK LİSANS TEZİ

İrem TOPAL
(509141104)

Fizik Mühendisliği Anabilim Dalı

Fizik Mühendisliği Programı

Tez Danışmanı: Doç. Dr. Cem SERVANTIE

AĞUSTOS 2017

İrem TOPAL, a M.Sc. student of ITU Graduate School of Science Engineering and Technology 509141104 successfully defended the thesis entitled "MOLECULAR DYNAMICS STUDY OF THE THERMAL CONDUCTIVITY IN NANOFLUIDS", which he/she prepared after fulfilling the requirements specified in the associated legislations, before the jury whose signatures are below.

Thesis Advisor :	**Assoc. Prof. Cem SERVANTIE** Istanbul Technical University	.....
Jury Members :	**Prof. Dr. Ekrem AYDINER** Istanbul University	.....
	Assoc. Prof. Ahmet Levent SUBAŞI Istanbul Technical University	.....
		.....

Date of Submission : **5 July 2017**
Date of Defense : **2 August 2017**

To my father,

FOREWORD

I would like to express my sincere gratitude, first and foremost, to my supervisor Assoc. Prof. Cem SERVANTIE, for his constant guidance, assistance, and encouragement.

With his wise comments and suggestions, Ekin KÜÇÜKSÖNMEZ made an invaluable contribution to this thesis. I owe him a debt of gratitude for his continuous support during my journey through molecular dynamics.

I would like to express my special thanks to my dear friends Eray TEMUR and Hande TINAS. They always let me think out loud in their company and never withhold their support from me in the course of my thesis work.

I am deeply grateful to my brother, Onur PUSULUK, for his guidance into the world of physics. He has always believed in me not only during the writing of this thesis but at every point in my life.

Finally, I am thankful to all who are still able to keep working, believing in the power and influence of education and science despite the current unfavorable political and social environment.

August 2017

İrem TOPAL
(Physics Engineer)

TABLE OF CONTENTS

Page

ABBREVIATIONS

MD	**:** Molecular Dynamics
EMD	**:** Equilibrium Molecular Dynamics
NEMD	**:** Non-Equilibrium Molecular Dynamics
FENE	**:** Finitely Extensible Non-Linear Elastic

SYMBOLS

$\mathbf{j}_\lambda$	**:** Heat flux
$\mathbf{Q}$	**:** Heat transfer
λ	**:** Thermal Conductivity Coefficient
$\mathbf{T}$	**:** Temperature
$\mathbf{t}$	**:** Time
α	**:** Thermal Diffusivity Coefficient
ρ	**:** Density
$\mathbf{c_v}$	**:** Specific heat at constant volume
$\beta_\mathbf{T}$	**:** Isothermal Compressibility
$\mathbf{E}$	**:** Energy
$\mathbf{m}$	**:** Mass
$\mathbf{v}$	**:** Velocity
$\mathbf{k_B}$	**:** Boltzmann's Constant
$\mathbf{V}$	**:** Volume
$\hbar$	**:** Planck's Constant

LIST OF TABLES

Page

LIST OF FIGURES

Page

MOLECULAR DYNAMICS STUDY OF THE THERMAL CONDUCTIVITY IN NANOFLUIDS

SUMMARY

Nanofluids are a new kind of fluid which contain well-dispersed nano-sized solid particles. They tend to have higher thermal conductivity than the bulk fluid in which they are mixed. In this work, the thermal conductivity of the bulk Lennard-Jones fluid and nanofluids at various volume fractions of nanoparticles is computed thanks to equilibrium molecular dynamics (EMD) and non-equilibrium molecular dynamics (NEMD) simulations. The Green-Kubo formalism is used for the EMD simulations while a net heat flux is imposed on the system with a change of the boundary conditions for the NEMD simulations.

The interactions inside the nanoparticles, between the fluid atoms, and between nanoparticles and fluid atoms are all taken as a Lennard-Jones potential. An empirical parameter, ζ, is added to the attractive part of the potential to control the hydrophilicity of the nanoparticles. Additionally, bonded atoms of nanoparticles interact with the Finitely Extensible Non-Linear Elastic (FENE) potential.

The NVE ensemble is used in the simulations, for which the total number of atoms, the total volume and the total energy are constant. In order to improve the computational efficiency, we construct neighbor lists with the cell list algorithm. The equations of motion are then integrated with the Velocity Verlet algorithm with a time step of 0.001. The total energy E and the total momentum P are computed to check the validity of the code since they are both conserved quantities. Using the Lennard-Jones phase diagram from literature, we choose a phase point corresponding to a liquid state. The temperature and density are taken respectively as 1.1 and 0.7798 in dimensionless units throughout all the simulations.

The initial condition of the bulk fluid has a total number of 5000 fluid atoms arranged in a regular FCC lattice. On the other hand, a spherical nanoparticle consisting of 58 atoms is generated and equilibrated in a separate molecular dynamics simulation. The bulk fluid and nanoparticles are mixed to obtain 4 simulation boxes with varying nanoparticle volume fractions of 2%, 3%, 6% and 10%. The hydrophobic parameter of the interaction potential between nanoparticles is fixed to $\zeta_{nn} = 0.3$ for all the simulations in order to prevent flocculation, and thus to have a well dispersed nanofluid. On the other hand, in order to study the effect of hydrophilicity on the thermal conductivity we use three different values of the hydrophilicity parameter of the fluid-nanoparticle interaction, namely $\zeta_{nf} = 0.5$, $\zeta_{nf} = 1$ and $\zeta_{nf} = 1.5$. In total 12 sets of simulations are initially run for 10^7 time steps of equilibration. The resulting coordinates are then used for the calculation of the average kinetic and potential energies of each atom of each species for a further 10^6 time steps. Finally, molecular dynamics simulations for collecting the heat current data are computed during 10^7 time

steps. The time auto-correlation function of the heat current and its time integral are calculated in a post-processing program.

The results show that the hydrophilicity of the nanoparticles did not have a measurable effect on the thermal conductivity of the nanofluid. Nanofluids with volume fractions of 2% and 3% showed an enhanced thermal conductivity with respect to the bulk fluid. The increase in the thermal conductivity is of approximately 10%. Surprisingly, nanofluids with higher volume fractions did not show any enhancement of the thermal conductivity. The numerical results obtained from EMD are then validated with NEMD simulations.

NANOAKIŞKANLARDA TERMAL İLETKENLİĞİN MOLEKÜLER DİNAMİK HESAPLAMALARI

ÖZET

Termal sistemlerin gelişmesi ile birlikte enerjinin etkin ve verimli kullanılması üzerine yapılan çalışmalar yoğunluk kazanmıştır. Endüstrinin hemen her alanında kullanılan elektronik cihazların performanslarına paralel olarak ürettikleri ısı artmakta ve bu ısıyı sistemden uzaklaştıran soğutma sistemlerinin iyileştirilmesi önemli bir problem olarak ortaya konmaktadır.

Nanometre mertebesinde metalik veya metalik olmayan katı parçacıklar içeren kararlı akışkan karışımları nanoakışkan olarak adlandırılır. Nanoteknolojinin bu denli ilerlemesinden önce çoğunlukla mikron mertebesinde parçacıklar içeren akışkanlar çalışılıyordu ancak bu parçacıklar büyüklükleri sebebiyle çökelme, tortulaşma ve aşınma gibi problemlere sebep oluyordu ve bu durum mühendislik uygulamalarında tehlikelere yol açıyordu. Nanometre mertebesinde parçacıkların üretilebilmesi ve çalışılabilmesi sonucu yayımlanan çalışmalar bu kolloid süspansiyonların ısıl iletkenliklerinin geleneksel ısı transferi akışkanlarına göre daha yüksek olduğunu gösterdi. Bu ısı transferini iyileştiren performansları sayesinde nanoakışkanlar on yılı aşkın bir süredir mühendislik uygulamalarında oldukça geniş bir yelpazede çalışılmaktadır. Nanoakışkanların artan ısıl iletkenliklerinden ve bu durumun arkasındaki fiziğin daha iyi anlaşılmasından yararlanan alanlar başlıca otomotiv sanayii, elektronik cihazların ekranları, gelişmiş minyatür kamera lensleri, kişisel bilgisayarlar, buzdolapları ve eşanjörler olarak sıralanabilir.

Literatürde deneysel ve ampirik çalışmaların yanı sıra, nanoölçekteki enerji taşınımının temel mekanizmasını anlamayı amaçlayan nümerik nanoakışkan çalışmaları da vardır. Ayrıca nanoakışkan üretiminin pratik ve finansal zorluğu, literatürdeki deneyler arasındaki uyuşmazlık ve kullanılan deneysel tekniklerin çeşitliliği gibi sebepler, nanoakışkanlar hakkında kapsamlı bir nümerik modellemeyi ilgi çekici de kılmaktadır. Bu nanoakışkan çalışmasında da moleküler dinamik metodları ile elde edilen nümerik sonuçlar sunulmaktadır.

Moleküler dinamik yöntemi, analitik olarak çözülemeyen çok parçacıklı sistemlerin hareket denklemlerini, klasik fizik yasalarını kullanarak bilgisayar ortamında nümerik metodlarla çözme yöntemidir. Etkileşim potansiyelinden her bir atom üzerine etki eden net kuvvetin bulunması ve atomların belirli bir zaman içindeki yörüngelerinin, Newton'un ikinci hareket yasası ile hesaplanması esasına dayanır. Simülasyonlar sonucunda sistemin tüm termodinamik ve mekanik özellikleri istatistiksel mekanik bağıntıları ile hesaplanabilir. Tıpkı deneysel çalışmalardaki gibi, önce N parçacık içeren model sistem seçilir ve örnek hazırlanır. Termal dengeye geldikten sonra gereken ölçümler alınır. Bu tip bir moleküler simülasyonda karşılaşılabilecek, modelin yanlış hazırlanması, yeterince uzun süre ölçüm alınmaması veya ölçmek istediğimiz niceliği ölçmüyor olmak gibi sorunlar deneysel çalışmalardaki gibi hatalara sebep olabilir.

Bu çalışmada, tüm parçacıklar arasındaki etkileşim için, moleküler simülasyonlarda en çok kullanılan matematiksel model olan Lennard Jones potansiyeli kullanılmıştır. Etkileşim potansiyeli parametreleri için indirgenmiş moleküler dinamik birimleri kullanılarak, baz akışkan olarak en genel Lennard Jones akışkanı modellemek amaçlanmıştır. Tüm parçacıklar arasındaki etkileşime ek olarak, küresel olarak tasarlanan nanoparçacıkların içindeki komşu atomları arasına FENE potansiyeli uygulanmıştır. Tüm simülasyonlar Lennard Jones akışkanı faz diyagramından yararlanılarak önceden belirlenen bir yoğunluk ve sıcaklık değerinde gerçekleştirilmiştir. Bu değerler belirlenirken sadece sıvı fazında bir nokta olması dikkate alınmıştır. Simülasyonlar boyunca toplam atom sayısı, sistemin hacmi ve sistemin toplam enerjisinin korunduğu mikrokanonik kümede çalışılmıştır. Hesaplama zamanını kısaltabilmek, birbirinden çok uzaktaki atomların etkileşimini yoksaymak için bir kesme mesafesi verilmiş ve sadece bu mesafe içinde kalan atomlar için kuvvet hesabı yapılmıştır. Atomların yörüngelerini belirleyebilmek için integrasyon algoritması olarak Velocity Verlet kullanılmıştır.

Nanoparçacıkların sıvı içinde iyi dağıldığı bir nanoakışkan elde etmek, topaklanmanın önüne geçmek için farklı nanoparçacıkların atomları arasındaki Lennard-Jones potansiyelinin çekici kısmına hidrofobik bir katsayı eklenmiş ve bu katsayı tüm simülasyonlar boyunca sabit tutulmuştur. Bu katsayı sabit tutulurken, nanoparçacık atomları ile sıvı atomları arasına uygulanan Lennard-Jones potansiyelinin çekici kısmına eklenen ampirik katsayılarla, nanoparçacığın hidrofilik veya hidrofobik özellikler kazanması amaçlanmıştır. Bu şekilde nanoakışkanın hidrofobik etkileşimlerden hidrofilik etkileşimlere geçişinin ısıl iletkenliğe etkisi gözlenmek istenmiştir. Üç farklı katsayı ile modellenen bu etkileşimlerin tümünde hacimce %2, %3, %6 ve %10 katkı oranlarında nanoparçacık eklenmiş nanoakışkan kullanılmış ve nanoparçacıkların hacimsel katkısının ısıl iletkenliğe etkisi araştırılmıştır.

Farklı hacimsel katkılardaki 4 nanoakışkan modeli ve 3 farklı etkileşim potansiyeli için toplam 12 set hazırlanmış ve simülasyonlar 10^7 adım çalıştırılarak, denge konumları elde edilmiştir. Mikroskopik ısı akısı formülündeki her bir atomun ortalama enerji değeri baz akışkan durumunda tüm atomlar özdeş olduğu için sistemin toplam enerjisi atom sayısına bölünerek hesaplanmıştır. Nanoakışkan modellerinde, diğer bir deyişle çok bileşenli sistemlerde, atomların ortalama enerjileri bu şekilde hesaplanamaz. Bileşenler bazında ortalama almak da nanoparçacık atomları için yeterince hassas olmayacaktır. Nanoparçacık içinde çok komşusu olan bir atomun üzerindeki toplam kuvvet ile yüzeye yakın az komşulu bir nanoparçacık atomunun üzerindeki toplam kuvvet farklı olacağı için, ortalama enerji hesabı etkilenecektir. Bu nedenle, denge konumlarından başlatılan 10^6 adımlık simülasyonlarla her bir atomun kinetik ve potansiyel enerjilerinin zaman ortalaması alınmış ve tüm simülasyonlarda bu ortalama enerji değerleri kullanılmıştır. Mikroskopik ısı akısı hesapları için 5 10^5 dengeleme sonrasında başlatılan 10^7 adımlık moleküler dinamik simülasyonları çalıştırılmıştır.

Taşınım katsayıları akışkanların dinamik özelliklerindendir ve sistemin zamana bağlı davranışlarını tanımlarlar. Bu çalışmada denge durumundaki nanoakışkanın ısıl iletlenlik katsayısı hesaplanmaktadır. Durgun akışkanlarda ısı geçişi iletim formunda gerçekleşir, dolayısıyla Fourier Yasası ile ifade edilir. Isıl iletlenlik katsayısı sistemin ısıl dalgalanmalarına göre enerjinin nasıl taşındığını gösterir. Denge durumundaki moleküler dinamik simülasyonları ile ısıl iletkenlik Green Kubo bağıntısı ile hesaplanır. Bu çalışmada da, mikroskopik ısı akısının zaman

oto-korelasyon fonksiyonunun integraline dayanan bu yöntem ile önce baz akışkanın, daha sonra hacimce %2, %3, %6 ve %10 katkı oranlarında nanoparçacık eklenmiş nanoakışkanların ısıl iletkenliği değerlendirilmiştir.

Hidrofobik etkileşimlerin değerlendirildiği simülasyon sonuçlarında nanoparçacıkların kümelendiği gözlenmiş olup, iki farklı katsayı ile değerlendirilen hidrofilik etkileşimler ile iyi dağılmış nanoparçacıklardan oluşan nanoakışkanlar elde edilmiştir. Kümelenmenin yanında, hidrofilik durumlar için nanoparçacıklar etrafındaki radyal dağılım fonksiyonları hesaplanarak, nanoparçacık etrafındaki sıvı atomlarından oluşan katmanın da ısıl iletkenliğe etkisi araştırılmıştır. Nanoakışkan modellerinin tümünde kullanılan ampirik katsayıların ısıl iletkenlik katsayısına etkisinin olmadığı belirlenmiştir.

Nanoparçacıkların hacimsel katkısının ısıl iletlenliğe etkisi baz akışkanın ısıl iletkenliği ile karşılaştırılarak değerlendirilmiştir. %2 ve %3 hacimsel katkı oranlarında nanoparçacık içeren nanoakışkanlarda ısıl iletkenliğin yaklaşık %10 civarında arttığı, daha yüksek hacimsel katkılarda ısıl iletkenliğin değişmediği belirlenmiştir.

Denge durumu moleküler dinamik simülasyonları ile elde edilen sonuçlar, literatürde karşılaştırılabilecek deneysel veri olmadığı için, denge dışı moleküler dinamik simülasyonları ile elde edilen sonuçlarla doğrulanmıştır. İki yöntemle de bulunan ısıl iletkenlik değerleri uyumludur.

1. INTRODUCTION

1.1 Nanofluids

Heat transfer has a vital role in many areas such as power generation, air conditioning, transportation and microelectronics due to processes like heating and cooling. There are commonly used fluids in heat transfer devices for heating and cooling applications, thermal conductivities of these working fluids are one of the main parameter of heat transfer. Improving the efficiency of heat transfer devices leads to reducing the size of devices and decreasing the operating costs of them. Thus it is of interest to enhance the thermal conductivities of these working fluids. Adding solid particles into the fluids is one of the techniques in order to achieve this aim because of higher thermal conductivities of solid materials [1].

Nanofluids are a new kind of fluids which contain well dispersed nano-sized solid particles. Although, micron-sized particles in a liquid have been studied commonly they have corrosion and erosion hazards because of their sizes in engineering applications. After the advent of nanotechnology, it was observed that, nanofluids could form stable systems against colloidal suspensions with micron-sized particles [2]. It also have been indicated that, nanofluids tend to have higher thermal conductivity than the bulk fluids [3]. For this reason, it is important to study the physical properties of nanofluids [2]. On the other hand, nanofluids present the advantage to study the thermodynamics and transport properties with higher level of control by varying the volume fraction, size and particle properties [4, 5].

There is still no definitive theory on nanofluids [2]. In comparison with solid-solid composites or conventional colloid suspensions nanofluids have different thermal behaviour. For example, smaller grain size of a constituent leads to reduced thermal conductivity in standard solid-solid composites while smaller nanoparticle leads to increased thermal conductivity in nanofluids. The physics behind nanofluids needs

a multidisciplinary understanding since it requires perspectives from the material science, chemistry and engineering [6, 7].

There are three approaches for nanofluids study: experimental, empirical and numerical. Since 1993, the number of experimental works has been increasing [6]. Empirical works on nanofluids can be considered as case dependent because of the lack of understanding of the energy transport mechanism at the nano-scale. Published numerical works tend to oversimplify the physics behind the thermal transport properties of nanofluids. For instance, as in our case, some of these works use a simple potential to model a nanofluid and there is no experimental data in the literature for validating such numerical studies [2].

Both experimental works, which are giving some properties of nanofluids correctly, and empirical works, which are fitting data to experiments, do not provide a basic microscopic understanding of heat transfer mechanisms in nanofluids. The practical difficulties in producing nanofluids, the large diversity of experimental techniques and the substantial discrepancies among these experiments motivated scientists for studying nanofluids with detailed numerical models so that fundamental questions could be answered [2].

Many branches of science and engineering are interested in studying thermodynamics properties of multicomponent mixtures with EMD [2]. Various important points of view are not clear because of the limits of the works in these fields [8]. One can not understand solid-fluid interactions in nanofluids without an inclusive understanding of the physics at the nano-scale [2].

1.2 Thermal Conductivity

Heat is defined as the form of energy transferred from a system at higher temperature to one at a lower temperature. The science of heat transfer focuses on the dynamics of such energy exchanges [9].

The rate of heat transfer per unit area normal to the heat transfer direction is called heat flux and expressed as,

$$\mathbf{j}_\lambda = \frac{\dot{Q}}{A} \tag{1.1}$$

where $\dot{Q}$ is the heat transfer rate and A is the heat transfer area [9].

Thermal conduction is one of the mechanisms of heat transfer, it is based on the energy transfer from particles with higher energy to less energetic ones due to the interactions between them. Interactions mean the collisions of the particles in liquids and gases [9]. The equation known as Fourier's law of heat conduction that relates the heat flux to the temperature gradient is expressed as:

$$\mathbf{j}_\lambda = -\lambda \nabla T \tag{1.2}$$

where λ is the thermal conductivity coefficient which measures the ability of a material for heat conduction. The units of λ are $[\frac{W}{mK}]$ [10]. Heat conduction is in the direction of decreasing temperature so the temperature gradient becomes negative. The negative sign is used in the Eq. (1.2) so that heat transfer can be a positive quantity [9]. The consequence of Fourier's law of heat conduction is the heat equation and is given,

$$\frac{\partial T}{\partial t} = \nabla(\alpha \nabla T) \tag{1.3}$$

where $\alpha = \frac{\lambda}{\rho c_v}$ is thermal diffusivity coefficient. The heat equation described by a partial differential equation has a vital position in modern mathematical physics. It was formulated and published by Jean Baptiste Joseph Fourier. After this publication, the equation and the solution method implemented various problems in many fields such as electricity, chemical diffusion, genetics and economics. Also, it should be mentioned that, the developments leading up to Fourier's work were critical for modern science [10].

The invention of thermometers played a critical role in the development of the science of heat, because there was no attempt to measure heat independently of temperature during this development of thermometer period [10, 11]. In 1597, Galileo invented a primitive form of the thermometer, called thermoscope, which works on the principle of changing density of a fluid depending on its temperature. In 1701 Newton contributed to improving the scale with his published work. Newton's scale was based on his own experimental results. According to his experiments, he established his scale by taking the boiling points of liquids and the melting and freezing points of metals and alloys as fixed points [11]. Fahrenheit, a German physicist, adopted the scale now known by his name, in 1724 [10].

Aside from the developments in the concept of heat, one should note the developments in the theory of ordinary and partial differential equations. In 1752, Bernoulli

used trigonometric series for solving differential equation that describe a vibrating string. Moreover, d'Alembert, Euler and Lagrange contributed to these mathematical developments by similar usage of trigonometric series leading to convergence issues and periodicity of these series [10].

In 1760, Joseph Black noticed that the temperature of ice does not change when it melts, he also observed that different amounts of heat are needed to raise the temperatures of different substances at equal masses. The discovery of 'latent heat' and 'specific heat' was the next important development after the establishing Fahrenheit scale [10]. Latent heat can be defined as the internal energy which is associated with the phase transitions in a system, and specific heat is the energy required per unit mass of a substance to increase its temperature by one degree [9].

Lavoisier and Laplace invented the first calorimeter in 1783, by measuring the latent heat of melting of ice and the specific heat of various materials. They conducted all the measurements taking water as reference. The specific heat had a significant role for understanding time-dependent changes of temperature leading to an essential component of the foundations of thermodynamics [10].

Another critical development was the work of Jean Baptiste Biot on the problem of heat conduction in 1804. He observed that, in a rod heated at one end, heat was also lost to the atmosphere transverse to the direction of conduction. Then, mathematical description of heat conduction formed into a many-body problem [10].

The nature of heat was still under debate during the late nineteenth century. It was thought that heat was an invisible fluid called *"caloric"* since the early nineteenth century [10].

All these scientific developments set the stage for Fourier's contribution which has historical importance on thermal conductivity [10]. A complete scientific definition of conductivity was given by Fourier for the first time [12]. The nature of heat was still unclear when he started working on heat conduction problem. Firstly, Fourier idealized the behaviour of matter at the macroscale and avoided the discussion on the nature of heat. The method of solution was the most critical part in Fourier's work. He was aware of the studies giving trigonometric series solution of Bernoulli, Euler and Lagrange. He used the method of separation of variables and obtained

infinite trigonometric series solutions called 'Fourier series' and also found integral solutions now called 'Fourier integrals' [10]. Fourier conducted his experimental and theoretical works entirely with solids even if he acknowledges that liquids have a thermal conductivity, too [11]. Fourier submitted his work with some results about heat conduction in a cylindrical annulus, a sphere and a cube to the French Academy in 1807. The publication of his work was delayed because his mathematical approach was not well received by the committee consisting of Laplace, Lagrange, Monge and Lacroix. Afterwards, Fourier expanded the work and published it by himself in 1822, with the title *"Théorie Analytique de la Chaleur"* (Analytic Theory of Heat) [10]. This work is viewed as one of the most important contributions to modern science by many. Fourier struggled for this mathematical description for several years and this definition of thermal conductivity lead up the developments of other physical properties such as electrical resistivity and molecular diffusion coefficient [12].

1.3 Thermal Conductivity of Nanofluids

In experimental studies of nanofluids, thermal conductivity is commonly measured by the transient hot-wire technique. Other methods used in measurements can be sorted as steady-state parallel-plate technique, temperature oscillation technique and optical beam deflection technique [1]. Thermal conductivity enhancement of nanofluids is observed experimentally by different research groups since 1993 [2]. These experimental studies reported that the thermal conductivity of nanofluids is affected by many parameters such as particle volume fraction, particle and base fluid material, size and shape of the particle, temperature and acidicity of the nanofluid [1].

The first experimental nanofluid study was performed by Masuda *et al.* in 1993 [13]. They measured the thermal conductivity of silica, alumina and other oxides in water and found an increase as 32.4% for the thermal conductivity of 4.3% particle volume fraction. They showed that increasing particle volume fraction linearly increase the thermal conductivity of nanofluids. In 1999, Lee *et al.* studied the thermal conductivity of ethylene glycol-based nanofluid with alumina particles, in addition to the water-based nanofluid [14]. They reported an enhancement of 20% for 4% particle volume fraction of the thermal conductivity and a linear increase with increasing volume fraction. Wang *et al.* investigated the thermal conductivity enhancement of

nanofluids, not only for particle volume fraction but also for the size of the nanoparticle [15]. They observed the same linear relationship between thermal conductivity and particle volume fraction and an increase of the thermal conductivity as decreasing the size of the particle. Eastman *et al.* found very significant increases in thermal conductivity, up to 40%, for particle volume fraction below one percent [16]. Thermal conductivity enhancement was steeper at low nanoparticle loading than higher loading according to their experiments.

The particle material is also investigated in most of the experimental studies as an important parameter for the thermal conductivity [1]. The study mentioned before conducted by Lee *et al.*, showed that nanofluids with CuO have better enhancement than the nanofluids with Al_2O_3, in opposition to what is expected since CuO has a smaller thermal conductivity than Al_2O_3 [14]. On the other hand, Chopkar *et al.* concluded that since Ag_2Al has higher thermal conductivity than Al_2Cu nanoparticle, nanofluids with Ag_2Al showed higher thermal conductivity than nanofluid with Al_2Cu according to their measurements [17].

Scientists have proposed many explanations for the thermal conductivity enhancement based on experimental data in the literature [2]. Brownian motion of the nanoparticles, clustering of the nanoparticles, liquid layering around nanoparticles and radiative heat transfer are the commonly proposed mechanisms to clarify thermal conductivity enhancement [1]. Random motion of nanoparticles in the bulk fluid is Brownian motion and this irregular motion causes transportation of energy by the nanoparticles. [1] Nanoparticle clustering in the fluid affects the thermal conductivity but its magnitude is still under debate [2]. Liquid layering around nanoparticles is proposed as a mechanism by some research groups, even though there is no experimental data about the thickness and thermal conductivity of these nanolayers [1]. Also, there are some studies regarding radiative heat transfer between the nanoparticles in the literature [2]. Some empirical models were derived by some authors to predict the thermal conductivity enhancement, while others assert for the conventional models such as Maxwell's theory and Hamilton-Crosser model [2].

According to some studies, experimental data showed little or no enhancement in the thermal conductivity of nanofluids [2]. Putnam *et al.* measured the thermal diffusivity of fluid mixtures and nanofluids with an optical beam deflection technique [18]. They

did not observe anomalous enhancement of the thermal conductivity of nanofluids with Au particles. They concluded that the maximum increase observed was $1.3\% \pm 0.8\%$ for Au particles. Zhang *et al.* measured the effective thermal conductivity and thermal diffusivity of various nanofluids by removing the influences of the static charge and electrical conductance of the nanoparticle, for an accurate measurement [19]. They concluded no anomalous enhancement on the effective thermal conductivity of the nanofluids. Buongiorno *et al.* performed an international nanofluid benchmark exercise by reproducing experimental data using classical effective medium theory for various nanofluids [20]. No significant enhancement in the thermal conductivity was observed by 34 different organizations.

There are very few numerical works of nanofluids in the literature [2]. Some of the most prominent numerical studies were performed by Sarkar *et al.* [21] and Li *et al.* [22]. They both modelled a copper nanoparticle in the liquid argon using EMD. They used the Lennard-Jones potential to model both the fluid and the particle. Sarkar *et al.* calculated the thermal conductivity of nanofluid using a single copper particle and tuning its volume fraction. They used the Green-Kubo formula and concluded that the thermal transport enhancement of nanofluids is mostly due to the increased movement of fluid atoms. Li *et al.* recorded the surrounding fluid atoms around spherical nanoparticle and determined the thickness of the nanolayer as approximately 0.5 nm. Water - Pt nanofluid is obtained based on a general MD modelling by Sankar *et al.* [23]. They used four different interactions to model a more realistic nanofluid. They noticed that the effective thermal conductivity of nanofluid increases proportionally with the temperature and volume fraction of the nanoparticle. Ghosh *et al.* calculated the thermal conductivity of water - copper nanofluids using a hybrid MD-stochastic model [24]. Their results agree well with the present experimental values reported in the literature. On the other hand, Xue *et al.* studied liquid layering effect on the thermal resistance by NEMD simulations [25]. They observed no effect on the thermal conductivity and suggested to rule out the explanation of liquid layering effect for the large enhancement of thermal conductivity in nanofluids. Keblinski *et al.* suggested that Maxwell's theory of well dispersed particles should be given up and allowed chain-forming morphologies for nanoparticles so that the disagreement between the experiment and the effective medium theory could be clarified [26]. They mentioned

the importance of aggregation on the thermal transport enhancement. Babaei *et al.* calculated thermal conductivity of different multi-component systems using EMD by comparing the results with the NEMD calculated results [27]. For well-dispersed nanofluid models, they did not observe any significant enhancement. They underlined the importance of correct definition of the average energies used in the heat current formula.

2. THEORY AND MODELLING

2.1 Transport Coefficients

The response of simple thermodynamic quantities to changes in variables like pressure or temperature are the thermodynamic response functions which are the second derivative of the thermodynamic potentials. These static properties of fluids are material dependent constants. For instance, the constant volume heat capacity c_v is the response to a change in temperature in the internal energy at constant volume and the isothermal compressibility β_T is the response to a change in pressure of the volume at constant temperature.

On the other hand, there are dynamic properties of fluids, such as thermal transport coefficients which measure the time dependent response to an external perturbation [28]. Gradients in concentration, velocity, temperature and electrical potential give rise to transport of mass, momentum, thermal energy and charge through the gas or fluid, respectively. The phenomena of diffusion, viscosity, thermal conductivity and electrical conductivity are called *"transport phenomena"*. They are all physically similar so a common mathematical formalism may represent them. Transport is formulated in a general form as:

$$\mathbf{J} = -\alpha \nabla \phi \tag{2.1}$$

where $\mathbf{J}$ is the flux vector which quantifies the transfer per unit area per unit time of the quantity ϕ and α is the transport coefficient which quantifies the resistance to the flow. The negative sign comes from the direction of transport which is from regions of high concentration to regions of low concentration [29]. Newton's law of viscosity, Fick's law of diffusion and Ohm's law of electrical conduction are examples to this phenomenological first order relation [28]. The transport properties of materials take an important place in many technical and natural processes. With the development of computing power, we can construct models to describe the transport properties in regions where experimental data are not available or strenuous to provide [30] .

The response of an equilibrium system to a small external thermal perturbation is described by the linear response theory; it defines generalized *"susceptibilities"* [31]. In NEMD, transport coefficients are determined by taking the ratio of a flux to the gradient which provides the driving force for the flux using linear response theory [32]. Since there is a gradient and a resulting flux, one can assume these laws can only be applied to nonequilibrium systems. However, the transport coefficients can be calculated also from EMD with the microscopic fluctuations of a system at equilibrium, as well as nonequilibrium situations [28]. To calculate transport coefficients using EMD, equilibrium time-correlation functions should be computed [32].

2.1.1 Time auto-correlation functions

If two different quantities A and B are correlated, then correlations between them are measured via the correlation coefficient c_{AB} defined as:

$$c_{AB} = \frac{\langle \delta A \delta B \rangle}{\sigma(A)\sigma(B)} \tag{2.2}$$

where

$$\delta A = A - \langle A \rangle_{ens} \tag{2.3}$$

and

$$\sigma^2(A) = \langle \delta A^2 \rangle = \langle A^2 \rangle_{ens} - \langle A \rangle_{ens}^2 \tag{2.4}$$

The absolute value of c_{AB} takes values between 0 and 1 according to the Schwartz inequalities. Values close to 1 point out a high degree of correlation. The correlation coefficient concept may be extended in a functional approach, by considering A and B to be evaluated at two different times. The resulting quantity $C_{AB}(t)$ is called a time correlation function and defined as:

$$C_{AB}(t) = \langle \delta A(t) \delta B(0) \rangle_{ens} \tag{2.5}$$

In the case of identical functions, $C_{AA}(t)$ is an autocorrelation function and measures how the values of A at two different times are correlated. In MD simulations, autocorrelation functions are of great interest, because their time integrals are directly related to the transport coefficients [33].

Transport coefficients characterise the response of a system to a perturbation. For instance, in our study, the thermal conductivity coefficient relates the heat flux to a temperature gradient. The infinite time integral of an equilibrium time autocorrelation function is of the form:

$$\gamma = \int_0^\infty dt \langle \dot{A}(t)\dot{A}(0)\rangle \tag{2.6}$$

where γ is the transport coefficient and A is a variable seen in the perturbation term in the Hamiltonian [33].

On the other hand, Einstein showed that there is a relationship between the transport coefficients, the diffusion coefficient of the Brownian motion, and the random walk [34]. The so called "Einstein Relation", which is expressed as,

$$2t\gamma = \langle (A(t) - A(0)^2)\rangle \tag{2.7}$$

which holds for large t in comparison to the correlation time of A [33]. According to the Einstein relation, each transport coefficient can be calculated from the linear increase of the statistical variance of the corresponding quantity [34]. There exist only a few genuine transport coefficients because only a few variables A give a non-zero γ according to the Eq.s (2.6) and (2.7). Transport coefficients may be calculated both from equations (2.6) and (2.7) [33], as stated in Table 2.1 with the corresponding phenomenological relation.

Table 2.1 : Generalized Einstein equations and corresponding Green-Kubo equations to calculate the transport coefficients.

Generalized Einstein relation	Green-Kubo relation	Phenomenological Law
$\frac{1}{2}\lim_{t\to\infty}\frac{d}{dt}\langle[G_D(t)-G_D(0)]^2\rangle$	$\int_0^\infty dt\langle j_D(t)j_D(0)\rangle$	$j_D = -D\nabla\rho$
$\frac{V}{2k_BT}\lim_{t\to\infty}\frac{d}{dt}\langle[G_\eta(t)-G_\eta(0)]^2\rangle$	$\frac{V}{k_BT}\int_0^\infty dt\langle j_\eta(t)j_\eta(0)\rangle$	$j_\eta = -\eta\frac{\partial v_x}{\partial z}$
$\frac{V}{2k_BT^2}\lim_{t\to\infty}\frac{d}{dt}\langle[G_\lambda(t)-G_\lambda(0)]^2\rangle$	$\frac{V}{k_BT^2}\int_0^\infty dt\langle j_\lambda(t)j_\lambda(0)\rangle$	$j_\lambda = -\lambda\nabla T$
$\frac{V}{2k_BT}\lim_{t\to\infty}\frac{d}{dt}\langle[G_\sigma(t)-G_\sigma(0)]^2\rangle$	$\frac{V}{k_BT}\int_0^\infty dt\langle j_\sigma(t)j_\sigma(0)\rangle$	$j_\sigma = -\sigma\nabla\phi$

2.1.2 Green Kubo relation for thermal conductivity

In 1960, fluctuating quantities were associated with each transport coefficients by Helfand. These fluctuating quantities are the centroids of the transported quantities and are called Helfand moments [34]. In the present work, the thermal conductivity

coefficient is the transport coefficient of interest. Energy is the transported quantity and the associated Helfand moment is given as the centroid of the energy fluctuations of the atoms

$$\mathbf{G}_\lambda = \frac{1}{V}\sum_{i=1}^{N}\mathbf{r}_i(E_i - \langle E_i\rangle) \tag{2.8}$$

where E_i is the energy per atom and is written as:

$$E_i = \frac{1}{2}m_i\mathbf{v}_i^2 + \frac{1}{2}\sum_{j\neq i}^{N}\mathscr{V}(r_{ij}) \tag{2.9}$$

where the first term is the kinetic energy and, the second term the total potential energy of atom i. Here, $\mathbf{v}_i$ and m_i represent the velocity and mass of the same atom. The potential energy of two atoms is taken to be divided equally between them. The thermal conductivity λ is given by

$$2t\lambda = \frac{V}{k_B T^2}\lim_{t\to\infty}\langle[\mathbf{G}_\lambda(t) - \mathbf{G}_\lambda(0)]^2\rangle \tag{2.10}$$

in terms of an Einstein relation [35]. On the other hand, for the corresponding Green-Kubo relation, the thermal conductivity coefficient λ is based on the integration of the time autocorrelation function of the heat current $\mathbf{j}_\lambda$

$$\lambda = \frac{V}{3k_B T^2}\int_0^\infty d\tau\langle\mathbf{j}_\lambda(\tau)\mathbf{j}_\lambda(0)\rangle \tag{2.11}$$

where T is the temperature of the system, V is the volume of the system and k_B is Boltzmann's constant. Both the Green Kubo relation and Einstein relation can be used for the calculation since they are equivalent

$$\lim_{t\to\infty}\frac{\langle[\mathbf{G}_\lambda(t) - \mathbf{G}_\lambda(0)]^2\rangle}{6t} = \int_0^\infty d\tau\langle\mathbf{j}_\lambda(\tau)\mathbf{j}_\lambda(0)\rangle \tag{2.12}$$

where the energy current is related to the Helfand moment by

$$\mathbf{j}_\lambda = \frac{d}{dt}\mathbf{G}_\lambda \tag{2.13}$$

Helfand moments are problematic with systems with periodic boundary conditions and should be modified to use in molecular dynamic simulations [34]. So, in this study, the Green Kubo formula will be used. The heat current can be evaluated as follows:

$$\mathbf{j}_\lambda = \frac{1}{V}\sum_{i=1}^{N}\left[\mathbf{v}_i(E_i - \langle E_i\rangle) + \mathbf{r}_i\frac{dE_i}{dt}\right] \tag{2.14}$$

where the time derivative of E_i:

$$\frac{dE_i}{dt} = \frac{d}{dt}\left(\frac{1}{2}m\mathbf{v}_i^2 + \frac{1}{2}\sum_{j\neq i}^{N}\mathscr{V}(r_{ij})\right) \tag{2.15}$$

$$= m\mathbf{v}_i.\mathbf{a}_i + \frac{1}{2}\sum_{j\neq i}^{N}\frac{\partial \mathscr{V}}{\partial \mathbf{r}_{ij}}.\frac{d\mathbf{r}_{ij}}{dt} \tag{2.16}$$

$$= \mathbf{v}_i.\sum_{j\neq i}^{N}\mathbf{F}_{ij} - \frac{1}{2}\sum_{j\neq i}^{N}\mathbf{F}_{ij}.(\mathbf{v}_i - \mathbf{v}_j) \tag{2.17}$$

$$= \frac{1}{2}\sum_{j\neq i}^{N}\mathbf{F}_{ij}.(\mathbf{v}_i + \mathbf{v}_j) \tag{2.18}$$

The force on atom i exerted by atom j is represented by $\mathbf{F}_{ij}$.

$$\mathbf{j}_\lambda = \frac{1}{V}\sum_{i=1}^{N}\mathbf{v}_i(E_i - \langle E_i\rangle) + \frac{1}{2}\frac{1}{V}\sum_{i=1}^{N}\mathbf{r}_i\sum_{j=1}^{N}\mathbf{F}_{ij}.(\mathbf{v}_i + \mathbf{v}_j) \tag{2.19}$$

$$= \frac{1}{V}\sum_{i=1}^{N}\mathbf{v}_i(E_i - \langle E_i\rangle) + \frac{1}{4}\frac{1}{V}\sum_{i=1}^{N}\sum_{j=1}^{N}[\mathbf{r}_i\mathbf{F}_{ij}.(\mathbf{v}_i + \mathbf{v}_j) + \mathbf{r}_j\mathbf{F}_{ji}.(\mathbf{v}_j + \mathbf{v}_i)] \tag{2.20}$$

The microscopic heat current takes its final form as:

$$\mathbf{j}_\lambda = \frac{1}{V}\left[\sum_{i=1}^{N}\mathbf{v}_i(E_i - \langle E_i\rangle) + \frac{1}{2}\sum_{i<j}^{N}\mathbf{r}_{ij}[\mathbf{F}_{ij}.(\mathbf{v}_i + \mathbf{v}_j)]\right] \tag{2.21}$$

2.2 Molecular Dynamics Simulations

The dynamics of microscopic particles are ruled by Schrödinger's equation,

$$i\hbar\partial_t\Psi = \mathscr{H}\Psi \tag{2.22}$$

where $\mathscr{H} = \mathscr{T} + \mathscr{V}$ is the Hamiltonian with $\mathscr{V}$ the interaction potential between the particles which depends on their positions [36].

Although the description of the dynamics of systems of atoms should be based on quantum mechanics, MD assumes a classical point of view. Indeed, at high enough temperature one can assume the system behaves classically. In this case, the dynamics are ruled by Newton's second law of motion

$$m_i\frac{d^2\mathbf{r}_i}{dt^2} = \mathbf{F}_i \tag{2.23}$$

Although the classical approach excludes quantum mechanical effects and the resulting chemical reactions, it has been proven successful for the calculation of macroscopic properties [36].

2.2.1 Interaction potentials

The Lennard-Jones potential was introduced by J.E. Lennard-Jones in 1924 to model soft-spheres. It is the most commonly used model among a number of semi-empirical expressions. Although it has been used for modelling liquid argon in most of the works, it also has been chosen as a general interaction potential for studies not involving specific substances, as in this work [28, 31]. The potential is defined as,

$$\mathscr{V}_{LJ}(r) = \begin{cases} 4\varepsilon\left[\left(\frac{\sigma}{r}\right)^{12} - \left(\frac{\sigma}{r}\right)^{6}\right] & \text{for } r < r_c \\ 0 & \text{for } r > r_c \end{cases} \tag{2.24}$$

where ε is the depth of the potential well, σ is the collision diameter for interacting particles and r is the separation between two interacting particles. The power 6 is chosen in accordance with the van der Waals forces regarding London forces and dipole-dipole interactions in quantum mechanics. 12 is chosen only for mathematical convenience independently of any physical basis [37]. The repulsive forces have a positive sign while the attractive forces a negative one [28]. The Lennard Jones potential can be used in systems which are in the solid, liquid or gaseous states [31].

The Lennard Jones interaction is truncated at a typical cutoff distance of $r_c = 2.5\sigma$ in dimensionless units for computational efficiency. For r_c is 2.5σ, the value of $\mathscr{V}_{LJ}(r)$ is -0.0163ε and the resulting force is $-0.039\varepsilon/\sigma$. From Fig. 2.1, it can be seen that the contributions to the force come from atoms at the cutoff distance is small, hence truncated version of the Lennard-Jones potential is used in our simulations. The truncated potential at r_c causes a truncated force leading to small impulses on atoms when their separation distance crosses r_c. Thus, small fluctuations in the total energy E can be observed instead of a constant E. A shifted potential and a resulting force applied at $r_c = 2.5\sigma$ is defined so that the energy fluctuations caused by the truncation of $\mathscr{V}_{LJ}(r)$ could be removed [28].

$$\mathscr{V}'_{LJ}(r) = \mathscr{V}_{LJ}(r) - \mathscr{V}_{LJ}(r_{cutoff}) \tag{2.25}$$

The forces are calculated from the interaction potential as,

$$\mathbf{F} = -\nabla\mathscr{V}_{LJ} \tag{2.26}$$

$$\mathbf{F}_{LJ}(r) = \begin{cases} \frac{24\varepsilon}{\sigma}\left[2\left(\frac{\sigma}{r}\right)^{13} - \left(\frac{\sigma}{r}\right)^{7}\right]\hat{r} & \text{for } r < r_c \\ 0 & \text{for } r > r_c \end{cases} \tag{2.27}$$

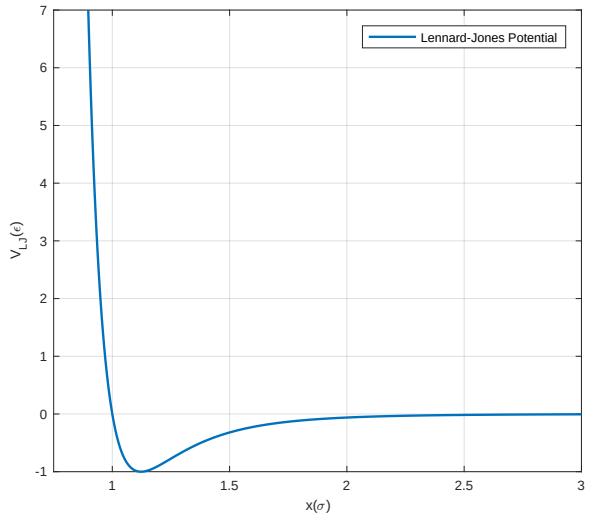

Figure 2.1 : Lennard-Jones Potential with $\sigma = 1$ and $\varepsilon = 1$.

In order to obtain a nanofluid, a spherical particle composed of 58 atoms is designed. The first atom is located at the origin and from this atom with a fix radius of 0.8σ and random angle values a spherical configuration is obtained in spherical coordinates. The nanoparticle's radius is determined to be 2σ. An equilibration process is performed for this initial configuration of the nanoparticle. Figure 2.2 shows the equilibrated nanoparticle used in the simulations.

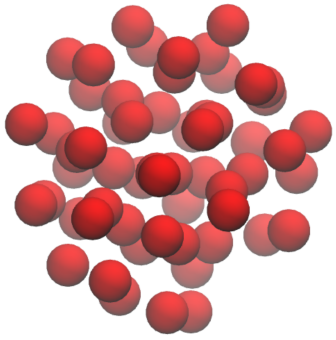

Figure 2.2 : Equilibrated nanoparticle.

The Lennard-Jones potential is applied between any two atoms of the nanoparticle. In addition, the Finitely Extensible Non-Linear Elastic (FENE) (Fig. 2.3) potential is added between two atoms of the nanoparticle which has a separation distance less than or equal to 1.5σ [38]:

$$\mathscr{V}_{FENE}(r) = \begin{cases} -\frac{1}{2}kR_0^2 \ln\left[1-\left(\frac{r}{R_0}\right)^2\right] & \text{for } r < R_0 \\ \infty & \text{for } r \geq R_0 \end{cases} \tag{2.28}$$

with $R_0 = 1.5\sigma, k = 30\varepsilon/\sigma^2$.

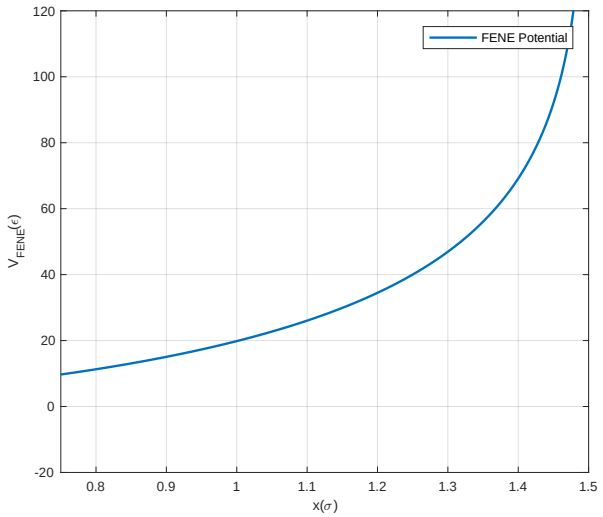

Figure 2.3 : FENE potential with $\sigma = 1$ and $\varepsilon = 1$.

The forces in the nanoparticle between bonded pairs are calculated from the interaction potential as,

$$\mathbf{F}_{FENE} = -\nabla \mathscr{V}_{FENE} \tag{2.29}$$

$$\mathbf{F}_{FENE}(r) = -\frac{kr}{1-(\frac{r}{R_0})^2}\hat{r} \tag{2.30}$$

The total potential for bonded atoms of nanoparticles is depicted in Fig. 2.4.

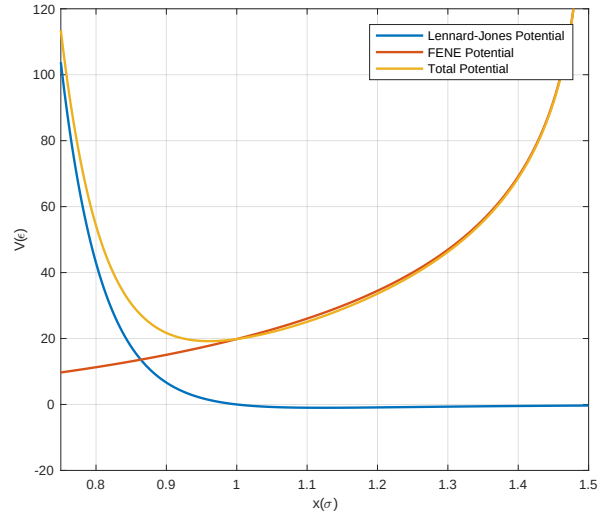

Figure 2.4 : Total potential with $\sigma = 1$ and $\varepsilon = 1$.

2.2.2 Interaction computations

The calculation of the forces acting on every particle for developing the simulations is the most time-consuming part, since the number of operation for the calculation of the forces scales as N^2 for a system of N particles because of the pair distance calculations [39]. A bookkeeping algorithm based on the determination of the atoms within the cutoff range from each atom can save time. Lists of neighboring atoms for each atom i, within a distance r_L of i are constructed in these algorithms [28]. Typically, r_L is larger than r_c and $r_L = r_c * 1.1 = 2.8\sigma$ in our study.

Cell subdivision is one of the techniques that reduces the computational effort from N^2 to $N \log N$. This technique is based on dividing the simulation region into small lattice cells which have edges of size r_c. Atoms are assigned to these cells according to their current positions so that the interaction between atoms could remain within the cells or the adjacent cells. In three dimensional systems, one must consider a total of 14 neighboring cells thanks to the third law of dynamics. Linked lists are formed to determine in which cell atoms reside in the cell list algorithm. Each cell has its own list [31]. This method is also much more efficient for large enough system [28].

There exist various numerical algorithms for integrating the equations of motion [31]. The Verlet algorithm is the simplest finite-difference method commonly used in molecular dynamics [28]. It can be derived with the combination of two Taylor expansions of the atoms coordinates and needs minimal memory storage which is a critical issue for large scale studies [31]. First, the Taylor series for position from time t to $t + \delta t$:

$$x(t+\delta t) = x(t) + \frac{dx(t)}{dt}\delta t + \frac{1}{2}\frac{d^2x(t)}{dt^2}\delta t^2 + \frac{1}{3!}\frac{d^3x(t)}{dt^3}\delta t^3 + O(\delta t^4) \tag{2.31}$$

Second, the Taylor series from time t to $t - \delta t$:

$$x(t-\delta t) = x(t) - \frac{dx(t)}{dt}\delta t + \frac{1}{2}\frac{d^2x(t)}{dt^2}\delta t^2 - \frac{1}{3!}\frac{d^3x(t)}{dt^3}\delta t^3 + O(\delta t^4) \tag{2.32}$$

Then, adding these two series expansions gives Verlet's algorithm for positions as:

$$x(t+\delta t) = 2x(t) - x(t-\delta t) + \frac{d^2x(t)}{dt^2}\delta t^2 + O(\delta t^4) \tag{2.33}$$

The velocity does not explicitly appear in the Verlet algorithm. If desired properties, such as kinetic energy, depend on velocity this may be problem. To overcome this problem and improve accuracy a related algorithm called Velocity Verlet is used. The Velocity Verlet scheme is simply [28],

$$x(t+\delta t) = x(t) + \frac{dx(t)}{dt}\delta t + \frac{1}{2}\frac{d^2x(t)}{dt^2}\delta t^2 + O(\delta t^3) \tag{2.34}$$

$$= x(t) + \delta t\left(\frac{dx(t)}{dt} + \frac{1}{2}\frac{d^2x(t)}{dt^2}\delta t\right) + O(\delta t^3) \tag{2.35}$$

$$= x(t) + \delta t\left(t + \frac{1}{2}\delta t\right)v + O(\delta t^3) \tag{2.36}$$

$$v\left(t + \frac{1}{2}\delta t\right) = v(t) + \frac{1}{2}a(t)\delta t + O(\delta t^2) \tag{2.37}$$

$$v(t+\delta t) = v\left(t + \frac{1}{2}\delta t + \frac{1}{2}\delta t\right) \tag{2.38}$$

$$= v\left(t + \frac{1}{2}\delta t\right) + \frac{1}{2}a(t)\delta t\left(t + \frac{1}{2}\delta t\right) + O(\delta t^2) \tag{2.39}$$

$$= v\left(t + \frac{1}{2}\delta t\right) + \frac{1}{2}a(t)\delta t(t+\delta t) + O(\delta t^2) \tag{2.40}$$

2.2.3 Initial conditions

In fact, the initial configuration does not have any effect when the equilibrium fluid state is studied. The ergodicity theorem states that one can derive meaningful data from the simulations if it is long enough [28]. The initial configuration of our bulk fluid system composed of 5000 atoms can be seen in Figure 2.5.

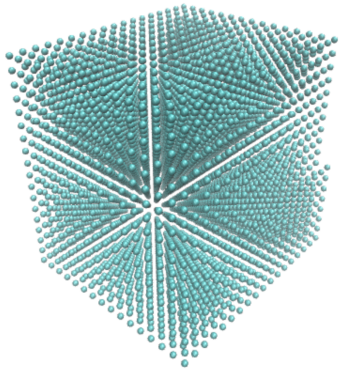

Figure 2.5 : Initial configuration of the bulk fluid.

The velocities are distributed as a Maxwell-Boltzmann distribution

$$\rho(\mathbf{v}_i) = \left(\frac{m}{2\pi kT}\right)^{3/2} \exp\left[-\frac{m}{2kT}(v_{ix}^2 + v_{iy}^2 + v_{iz}^2)\right] \tag{2.41}$$

which permits to initially fix the temperature of the system to the desired value. A velocity rescaling procedure before the run of the simulations is conducted for adjustment of the system temperature. Indeed, even though initially the temperature is at the desired value, the potential energy do not correspond to its equilibrium value, hence, the temperature will change [31].

2.2.4 Boundary conditions

If the simulations are carried out in a container of some kind and the walls of the container are like rigid boundaries that atoms collide when trying to escape from the simulation region, one will only observe surface effects. Indeed, in macroscopic systems, a very small fraction of atoms are close to a wall so surface effects are negligible in such kind of systems. For example, a system with $N = 10^{21}$ atoms has $N^{\frac{2}{3}} = 10^{14}$ atoms near to the walls, this means one in 10^7 atoms on the surface. On the other hand, for a more typical MD value of $N = 1000$, the number of atoms close to the walls is of order $1000^{\frac{2}{3}}$, roughly 500 atoms are near to the walls, very few atoms are in the bulk. Surface effects become important as the system size decrease. A simulation of such kind of systems give us information on the fluid near to solid surfaces instead of information on the behaviour of the bulk fluid. In order to study a system without any surface effect, periodic boundary conditions are implemented. The idea of periodic boundary conditions relies on identical copies of the simulation region so that an atom leaving the region through a particular bounding face could reenter the region through the opposite face, as seen in Figure 2.6 [31].

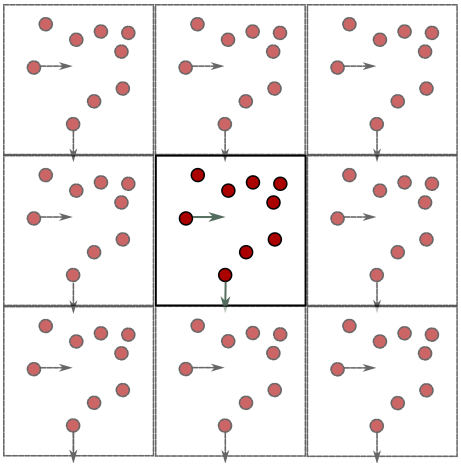

Figure 2.6 : Replication of the main cell in all directions.

The second consequence of this periodicity is that atoms within a distance r_c of a boundary interact with atoms in a neighboring copy of the system, as seen in Figure 2.7. It is obvious that after each integration step, periodic boundaries should be taken into account for examining the coordinates of an atom have moved outside the region to bring it back inside [31].

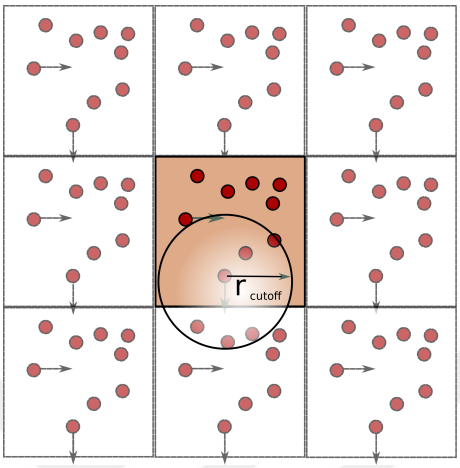

Figure 2.7 : Minimum image convention.

2.2.5 Technical details of the simulations

In the present work, a bulk Lennard-Jones fluid and nanofluids at various volume fractions of nanoparticles are modelled. The thermal conductivity of these model fluids is calculated using the Green Kubo formalism by EMD simulations.

The NVE ensemble is used where the total number of atoms, the system volume and the total system energy are constant. Force calculations are made only between the neighbors of an atom within a specified cutoff radius (r_c) equal to 2.5σ because of the negligible contribution of atoms at larger separations to the total force on a given atom. This is made with the Cell-list algorithm. Atomic trajectories are computed using the Velocity Verlet algorithm. From the Lennard-Jones phase diagram, a temperature and corresponding density value are specified by taking in consideration only the liquid phase region [40]. Temperature and density are taken as 1.1 and 0.7798 in dimensionless units throughout the simulations, respectively.

Initially, a total number of 5000 fluid atoms are arranged in a regular FCC lattice. The spherical nanoparticle consist of 58 atoms and approximately $r = 2\sigma$ radius in dimensionless units is constructed and equilibrated in a separate molecular dynamics

simulation before constructing the simulation boxes. First, 4 simulation boxes are prepared consisting of a single, 2, 4 and 6 identical nanoparticles and the fluid atoms. We define the volume fraction of the nanoparticles φ as,

$$\varphi = \frac{\frac{4}{3}\pi r_p^3}{V_{box}} \tag{2.42}$$

where r_p is the radius of the nanoparticle and V_{box} is the volume of the simulation box. In this work, for a single particle φ is found as 2%, for 2 particles φ is 3%, for 4 particles φ is 6% and for 6 particles φ is 10%.

In nanofluid models consisting of more than one nanoparticle, an empirical coefficient is used for the attractive part of the Lennard-Jones potential between the atoms of different nanoparticles in order to prevent the nanoparticles from flocculation. This coefficient is determined as $\zeta_{nn} = 0.3$ and fixed during all the simulations. The modified Lennard-Jones potential is defined as,

$$\mathscr{V}_{LJ}(r) = \begin{cases} 4\varepsilon\left[\left(\frac{\sigma}{r}\right)^{12} - \zeta\left(\frac{\sigma}{r}\right)^{6}\right] & \text{for } r < r_c \\ 0 & \text{for } r > r_c \end{cases} \tag{2.43}$$

Thanks to ζ we investigate how the transition of nanoparticles from hydrophobic interactions to hydrophilic interactions affects the thermal conductivity. For this purpose, three coefficients specified as $\zeta_{nf} = 0.5$, $\zeta_{nf} = 1$ and $\zeta_{nf} = 1.5$ are added to the attractive part of the Lennard-Jones potential between the nanoparticle atoms and the fluid atoms.

For four different nanofluid models and three different Lennard-Jones potential, in total 12 sets, we initially run 10^7 time steps to equilibrate the system. The resulting coordinates are then used for all the simulations.

To evaluate the average individual energies which are needed for the heat current calculation, in the case of bulk Lennard-Jones fluid, in other words single-component system, we use $\langle E_i \rangle = \frac{E_{total}}{N_{atom}}$ formula since all the atoms are identical. In nanofluid models, in other words multi-component system, atoms are not identical anymore and the average energies per atom can not be calculated in the same way. Moreover, as seen in Figure 2.8, the average energy of each atom in a nanoparticle is different, indeed, atoms in the nanoparticle which have much more neighboring atoms have larger energies with respect to atoms which have less neighboring atoms because of

the FENE potential. The time-average kinetic and potential energies for each atoms in each species are calculated as preliminary for 10^6 time steps.

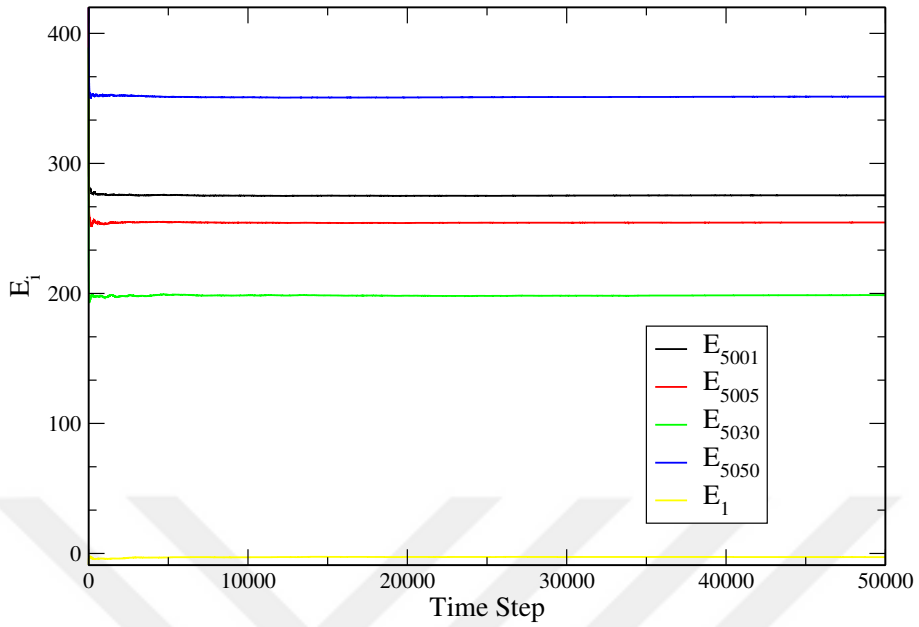

Figure 2.8 : Average energies of some nanoparticle and fluid atoms. Atom number 5001 has 18 neighboring atoms while atom number 5030 has only 2. Atom number 1 (a fluid atom) has lower average energy than the nanoparticle atoms.

Finally, molecular dynamics simulations for collecting the heat current data are started and continued for 10^7 time steps after 500000 time steps of thermal equilibration process. The integration time step is fixed to 0.001 for all the simulations. The integrated autocorrelation function of the equilibrium heat current is calculated in a post-processing program.

The MD codes are written in FORTRAN 90. The code is parallelized to reduce the calculation time with the openMP protocol and each simulation is performed with 4 processors.

2.2.6 Validation of the code

To verify if the MD code works correctly, the total energy E and the total momentum P are controlled, since they are conserved quantities in all MD simulations. The kinetic, the potential and the total energy are depicted in Fig. 2.9 (a). Since there are no external forces, $\sum_i \mathbf{F}_i = 0$, the total momentum is also conserved as seen in Fig. 2.9 (b).

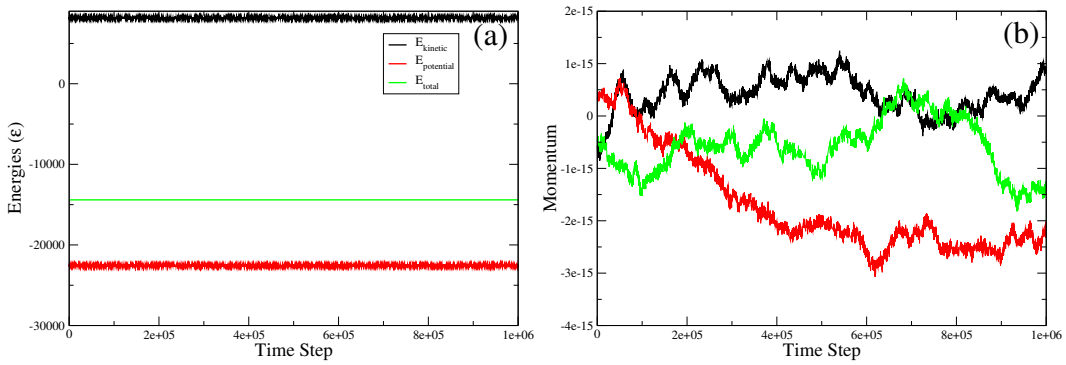

Figure 2.9 : (a) Energies of the bulk Lennard-Jones fluid. (b) The total momentum of the bulk Lennard-Jones fluid.

Fig. 2.10 is present a snapshot of nanofluid consisting 6 nanoparticles for $\zeta_{nf} = 1.5$ that we observe a well-dispersed nanofluid as an example.

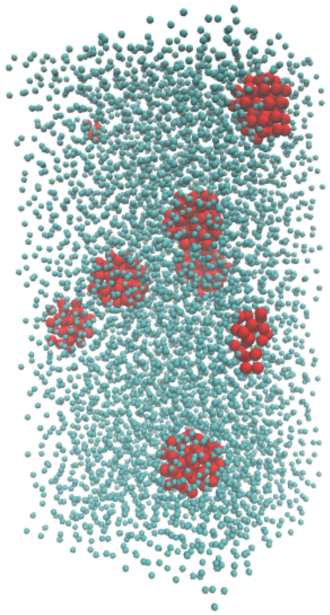

Figure 2.10 : Equilibrated nanofluid with 6 nanoparticles for $\zeta = 1.5$.

3. RESULTS

The results do not include the initial 500000 time steps run to reach thermal equilibrium for all the simulations. During the simulations, the heat current vector $\mathbf{j}_\lambda$ is computed at every time step thanks to Eq. (2.21). Then, the thermal conductivity of the bulk fluid and various nanofluids is calculated with Eq. (2.11) by EMD simulations and with Eq. (1.2) by NEMD simulations. Finally, the results of two methods are compared.

3.1 Thermal Conductivity of the Bulk Lennard-Jones Fluid

3.1.1 Equilibrium molecular dynamics simulations

The heat current for all the directions of the bulk Lennard-Jones fluid is plotted in Fig. 3.1. We see that the average flux is zero in each direction.

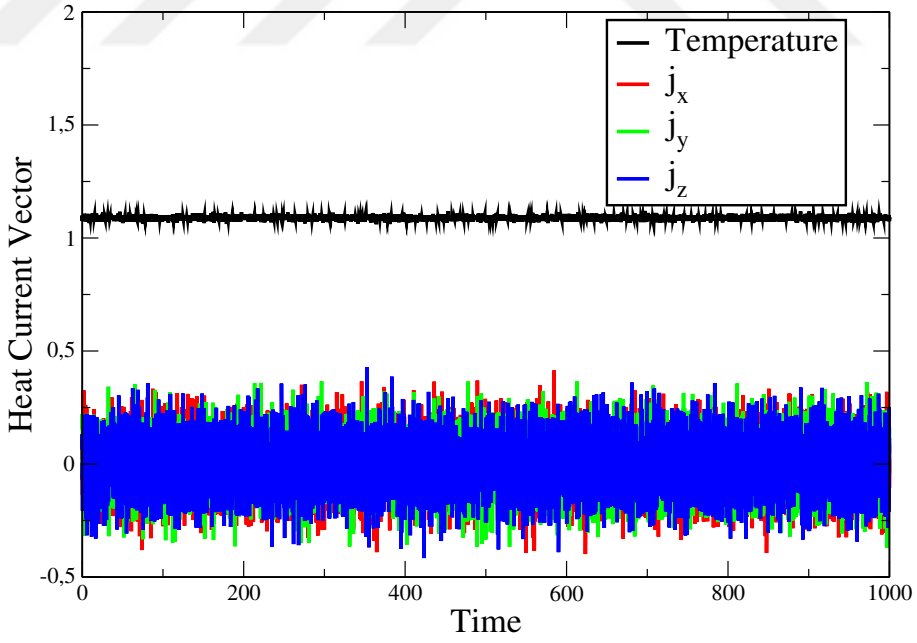

Figure 3.1 : Temperature and heat current for all three directions for the bulk fluid during an EMD simulation.

The heat current auto correlation function for the bulk fluid composed of 5000 atoms is depicted in Fig. 3.2. The time integral of the heat current auto correlation function gives the resulting thermal conductivity as seen in Fig. 3.2, the value of the thermal conductivity coefficient is found as approximately $\lambda = 6\ \frac{k_B}{\sigma^2}\sqrt{\frac{\varepsilon}{m}}$.

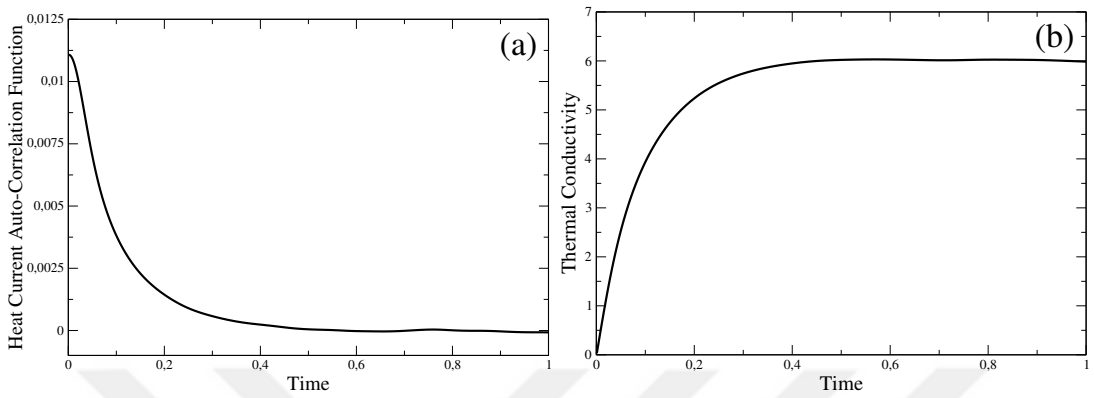

Figure 3.2 : (a)Decay of the heat current auto-correlation function and (b) integral of the heat current auto-correlation function of bulk Lennard-Jones fluid.

3.1.2 Non-equilibrium molecular dynamics simulations

Thermal conductivity coefficient λ calculated thanks to the Green-Kubo relation is compared with the results obtained from NEMD and Fourier's law. Statistical mechanics gives very little predictions when a system departs from equilibrium and MD begins to be important as an experimental tool. Modification of the boundaries is an approach for inhomogeneous systems. The stochastic walls method used in NEMD simulations is simply based on the reflection of atoms and modification of their velocities with a Maxwell-Boltzmann distribution corresponding to the temperature of the walls. After construction of the walls in $\hat{z}$ direction, we depict in Fig. 3.3 the heat flux for a difference in temperature $\Delta T = 1.5$ as an example. We observe that while $\langle \mathbf{j}_x \rangle = \langle \mathbf{j}_y \rangle = 0$ how $\langle \mathbf{j}_z \rangle$ has a negative value because the heat flow is downward.

A linear temperature profile is obtained by averaging the kinetic energies in small slices of 0.05σ as a function of z as seen in Fig. 3.4. Linear fits to the data gives the gradients of temperatures, ∇T, as a function of ΔT are depicted in Fig. 3.4.

The imposed heat flux is calculated in the same way as for the Green-Kubo method and the thermal conductivity coefficient λ is calculated using Fourier's law, we depict the thermal conductivity as a function of ΔT in Fig. 3.5. Both EMD and NEMD methods give consistent results.

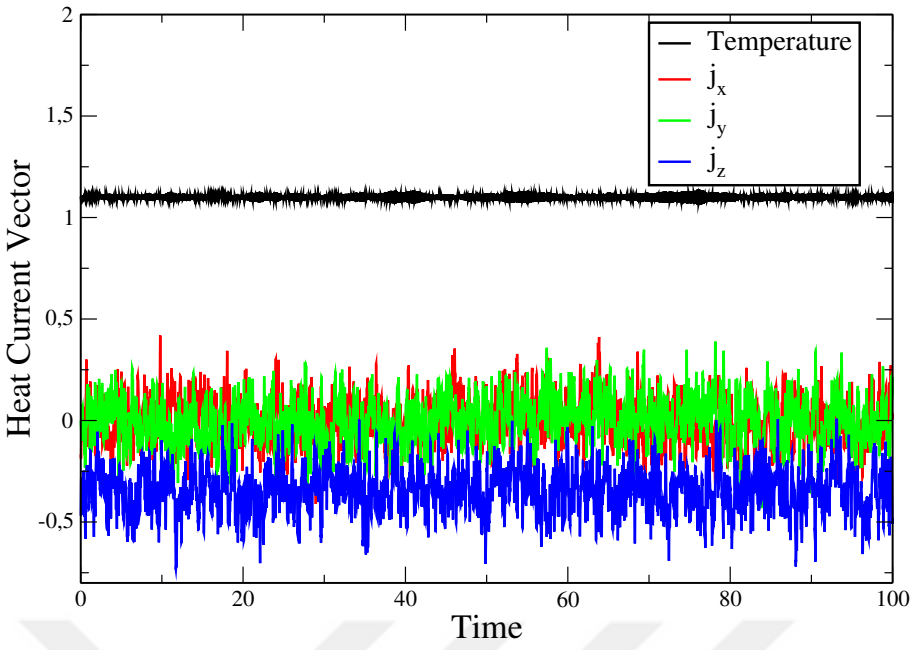

Figure 3.3 : Temperature and heat current for all three directions for the bulk fluid in the case of $\Delta T = 1.5$ during a NEMD simulation.

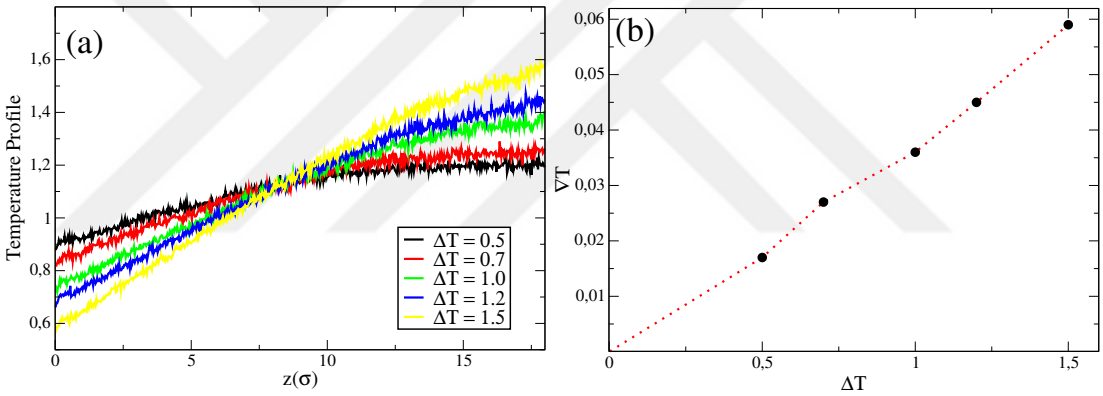

Figure 3.4 : The temperature profiles for various differences in temperature as a function of z (a) and resulting gradients of temperature (b).

3.2 Thermal Conductivity of Nanofluids

3.2.1 Equilibrium molecular dynamics simulations

3.2.1.1 The Effect of the particle-fluid interaction on the thermal conductivity

Figure 3.6 shows the thermal conductivities of nanofluids. In order to study the effect of the fluid density distribution around the nanoparticle on the thermal conductivity of a nanofluid, the thermal conductivity is evaluated for $\zeta = 1.0$ and $\zeta = 1.5$. In the case of more than one nanoparticle, $\zeta = 0.5$ is used to investigate the clustering effect

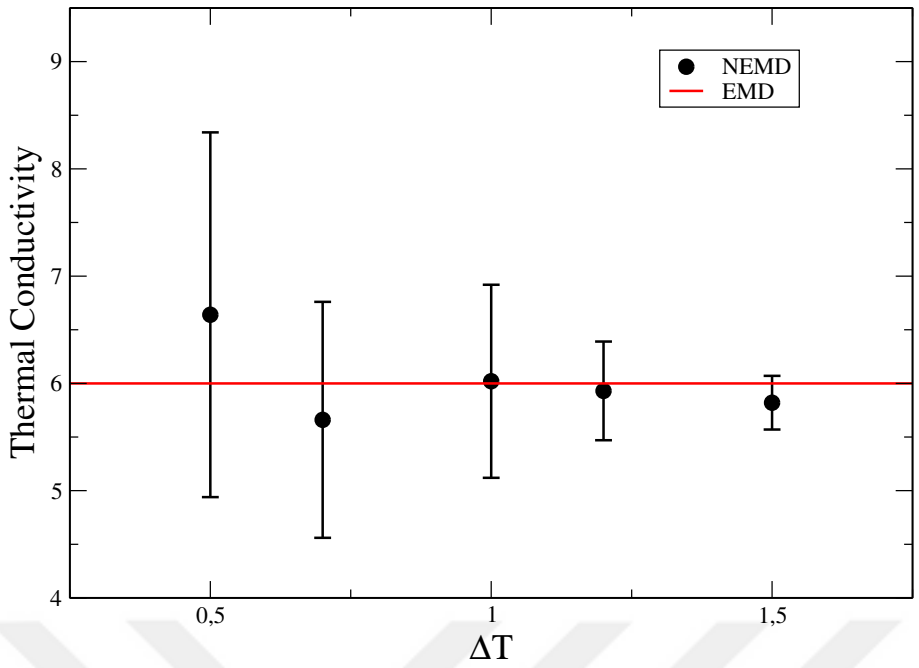

Figure 3.5 : The thermal conductivity coefficients calculated using Fourier's law for various differences in temperature.

on the thermal conductivity of nanofluids. The resulting thermal conductivities of the nanofluids containing 1, 2, 4 and 6 nanoparticles are depicted in Fig. 3.6, respectively. The thermal conductivity coefficients are calculated by averaging the data from 0.4 to 1. The thermal conductivity coefficient is found to be approximately 6.6 for a single nanoparticle and 6.7 for 2 nanoparticles in dimensionless units, slightly higher than the bulk fluid. The thermal conductivity of nanofluids containing 4 and 6 nanoparticles are found as 6 and 5.7.

We depict in Fig. 3.7 the radial distribution function of a nanoparticle for different values of the hydrophilic parameters ζ. We observe that the hydrophilic interactions between the particles and the fluid causes a layer to form around the nanoparticle depending on the power of the attractive forces. We can rule out the layering effect since the hydrophilic parameter do not have an observable effect on the thermal conductivity, as stated in the previous work by Xue *et al.* [25]. The results of all the nanofluid models demonstrate that there is no effect of particle-fluid interaction on thermal conductivity, except a slight increase for small volume fractions.

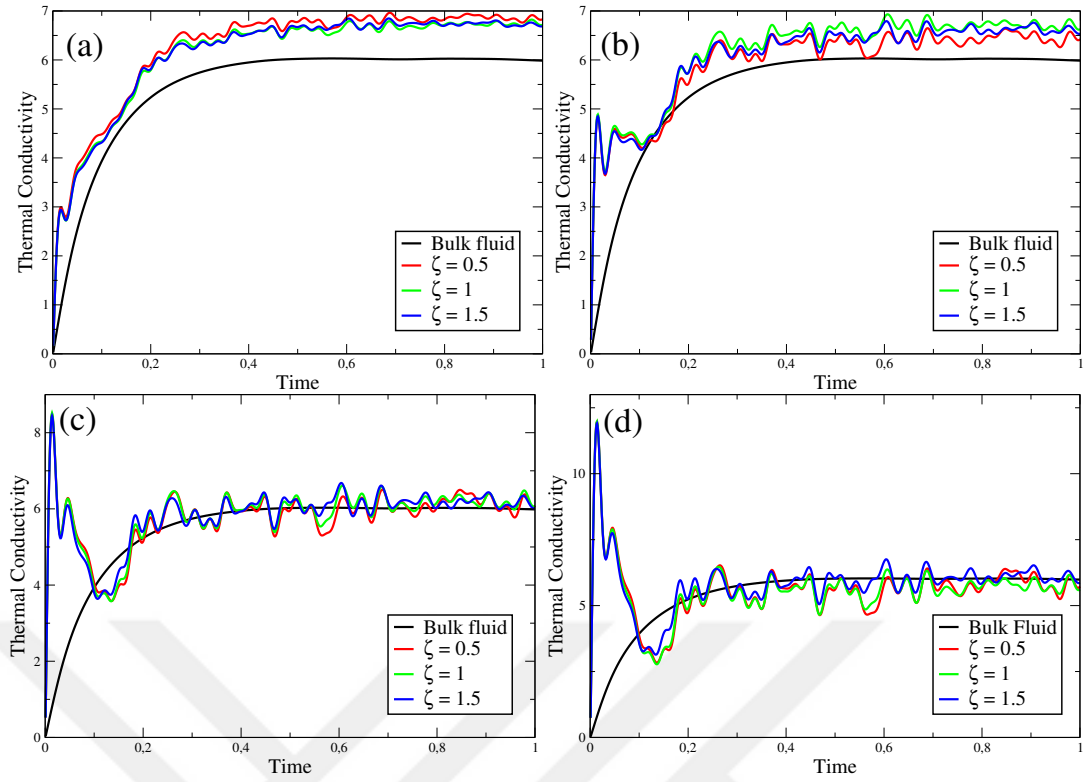

Figure 3.6 : Integral of the heat current auto-correlation function for various nanofluids.

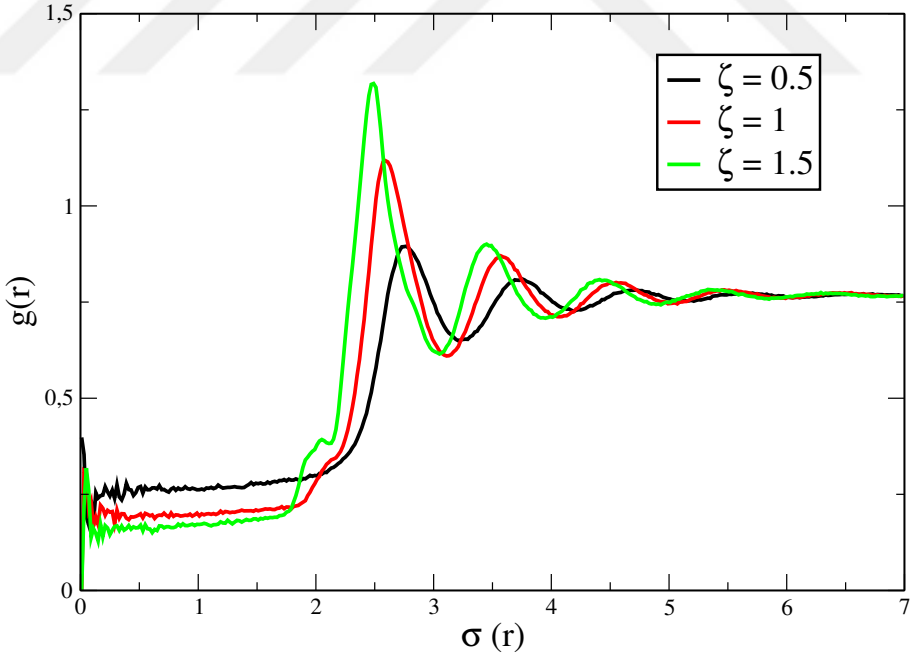

Figure 3.7 : Radial distribution function of a nanoparticle for different values of the hydrophilic parameter ζ.

3.2.1.2 Nanoparticle volume fraction effect on thermal conductivity

Since there is no effect of particle-fluid interaction on thermal conductivity, Fig. 3.8 is depicted in the case of $\zeta = 1$. The heat current auto-correlation functions of different nanofluids (Fig. 3.8) has an oscillationary behavior. We observe that with increased volume fraction of nanoparticles oscillation of the function is found to increase because of the long range correlations. For lower volume fractions (2% and 3%) the thermal conductivity is found to increase approximately 10% than the bulk fluid. For higher volume fractions (6% and 10%) the thermal conductivity do not show any enhancement. As stated before, these results are similar to the experimental data obtained by Eastman *et al.* [16].

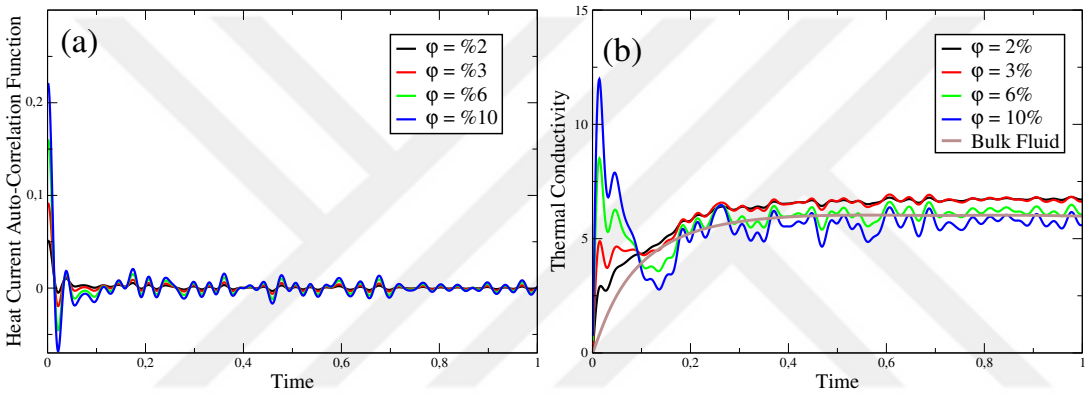

Figure 3.8 : Decay of the heat current auto-correlation functions (a) and integrals of the heat current auto-correlation functions of various nanofluids at different volume fractions (b).

3.2.2 Non-equilibrium molecular dynamics simulations

As in the case of the bulk Lennard-Jones fluid, the thermal conductivity of nanofluids are compared with NEMD simulations. We use the same stochastic walls to obtain a temperature gradient only for $\zeta = 1$ and $\Delta T = 1.5$ for nanofluids. It takes much more time to have the desired temperature in the bulk region and achieve a steady state with respect to the bulk case. The heat current vector and the temperature profile for the nanofluid with nanoparticle volume fraction 2% are depicted in Fig. 3.9, as an example.

The gradient of temperature is found to be as 0.025 by linear fit to the data in Fig. 3.9(b). Finally, Fourier's law gives the thermal conductivity as 6.24 $\frac{k_B}{\sigma^2}\sqrt{\frac{\varepsilon}{m}}$. The NEMD simulations are performed for the other nanofluid models in the same manner.

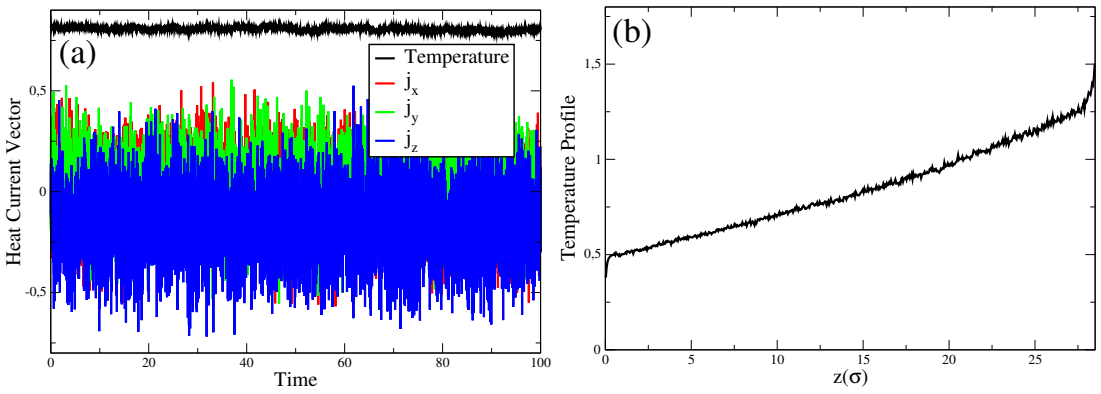

Figure 3.9 : (a)Temperature and heat current for all three directions for the nanofluid consisting 1 nanoparticle during a NEMD simulation. (b)The temperature profile for $\Delta T = 1.5$ as a function of z.

We depict the thermal conductivity as a function of the volume fraction obtained from both EMD and NEMD calculations in Fig. 3.10. The results of NEMD calculations are in agreement with the EMD within the error bars. The error bars are obtained by computing the statistical error on the expectation value of the heat flux, we note that the correlations are taken into account. As we observed before, except an increase for small volume fractions, namely 2% and 3%, we do not observe any enhancement of the thermal conductivity.

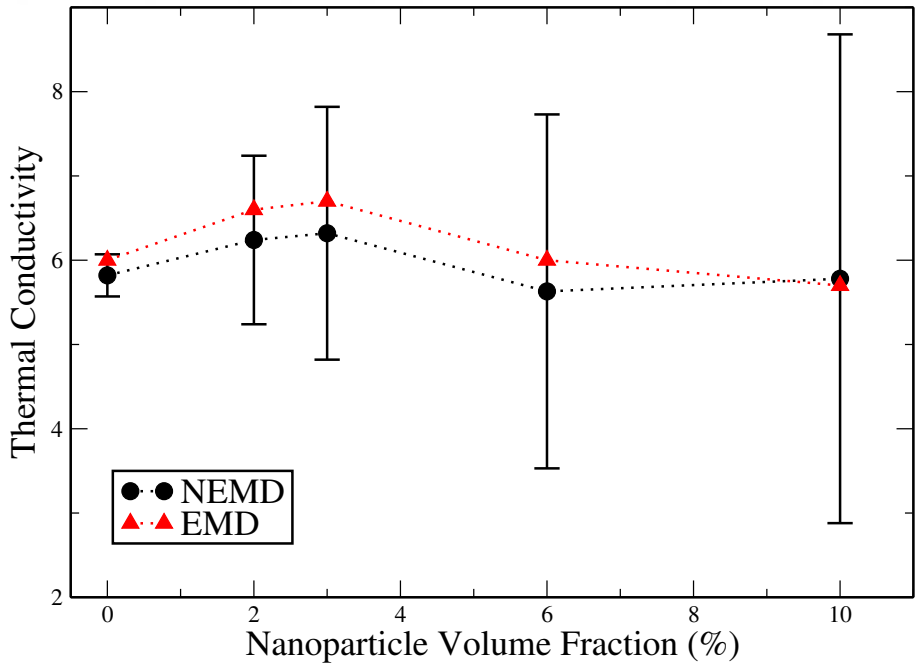

Figure 3.10 : Thermal conductivity as a function of the volume fraction of nanoparticle.

4. CONCLUSIONS

In this work we studied the thermal conductivity of nanoparticle and fluid composites. We modelled the base fluid with point particles interacting through Lennard-Jones interactions. The atoms inside the nanoparticles interact with a Lennard-Jones interaction, while the bonded pairs additionally interact with an attractive potential, the so called FENE potential. The nanoparticle-nanoparticle, and nanoparticle-fluid interaction are also Lennard-Jones interaction with an additional term to control the strength of the attractive part. Both EMD and NEMD were carried out for systems with different volume fractions of nanoparticles.

The results show that the effect of the hydrophilicity of the nanoparticles is negligible, indeed for three different values of the strength of the attractive part of the nanoparticle-fluid interaction we found the same thermal conductivity. This result is in agreement with previous works who ruled out the effect of liquid layering on thermal conductivity [25]. On the other hand, the computations show that for low volume fractions of nanoparticles $(2-3\%)$ there is an increase of the thermal conductivity of a maximum value of approximately 10% with respect to the bulk fluid. However, we did not observe any appreciable increase for higher volume fractions of nanoparticles. We remark that a similar observation was made by [16].

The lack of increase in the thermal conductivity of nanoparticle and fluid composites suggests that a number of previous numerical studies tend to over-estimate the conductivity of the nanofluid by an incorrect definition of the average energies of the atoms. Indeed, we observed very large increases of the conductivity when the average energies of the atoms of the nanoparticles were not carefully computed. We suggest that part of the discrepancies found in the literature could be due to this problem.

In order to confirm our results and find a reasonable explanation for the halt in the increase of the conductivity at higher volume fractions more extensive simulations are required. The size and shape of nanoparticles should be studied to rule out any system specific case and finite size effects. Electrostatic interactions should be taken into

account to quantify the importance of long range interactions. Finally, the influence of viscosity should be studied, indeed it is well known that the addition of nanoparticles to a base fluid can modify the viscosity.

REFERENCES

[1] **Özerinç, S.**, **Kakaç, S. and Yazıcıoğlu, A.G.** (2010). Enhanced thermal conductivity of nanofluids: a state-of-the-art review, *Microfluidics and Nanofluidics*, *8*(2), 145–170.

[2] **Puliti Gianluca**, **Paolucci Samuel and Sen Mihir** (2012). Nanofluids and Their Properties, *Applied Mechanics Reviews*, *64*(3).

[3] **Keblinski, P.**, **Eastman, J.A. and Cahill, D.G.** (2005). Nanofluids for thermal transport, *Materials Today*, *8*(6), 36–44.

[4] **Choi, S. and Eastman, J.**, (1995). Enhancing thermal conductivity of fluids with nanoparticles, volume231, ASME International Mechanical Engineering Congress and Exposition Proceedings, pp.99–105.

[5] **Saidur, R.**, **Leong, K. and Mohammad, H.** (2011). A review on applications and challenges of nanofluids, *Renewable and Sustainable Energy Reviews*, *15*(3), 1646–1668.

[6] **Das, S.**, **Choi, S.**, **Yu, W. and Pradeep, T.** (2007). *Nanofluids: Science and Technology*, Wiley.

[7] **Wang, L. and Fan, J.** (2010). Nanofluids Research: Key Issues, *Nanoscale Research Letters*, *5*(8), 1241.

[8] **Egorov, A.V.**, **Brodskaya, E.N. and Laaksonen, A.** (2006). Molecular dynamics simulations of solid–liquid phase transition in small water aggregates, *Computational Materials Science*, *36*(1–2), 166–170, proceedings of the Second Conference of the Asian Consortium for Computational Materials Science — ACCMS-2Second Conference of the Asian Consortium for Computational Materials Science.

[9] **Ghajar, A. and Cengel, Y.** (2014). *Heat and Mass Transfer: Fundamentals and Applications*, McGraw-Hill Education.

[10] **Narasimhan, T.N.** (1999). Fourier's heat conduction equation: History, influence, and connections, *Proceedings of the Indian Academy of Sciences - Earth and Planetary Sciences*, *108*(3), 117–148.

[11] **Burr, A.C.** (1933). Notes on the History of the Concept of Thermal Conductivity, *Isis*, *20*(1), 246–259.

[12] **Narasimhan, T.N.** (2010). Thermal conductivity through the 19th century, *Physics Today*, *63*(8), 36.

[13] **Masuda, H.E.A.T.K. and Hishinuma, N.** (1993). Alteration of Thermal Conductivity and Viscosity of Liquid by Dispersing Ultra-Fine Particles (Dispersions of c-Al 2 O 3 , SiO 2 , and TiO 2 Ultra-Fine Particles), *NETSU BUSSEI*, *7*(4), 227–233.

[14] **Lee, S.C.S.L.S. and Eastman, J.** (1999). Measuring Thermal Conductivity of Fluids Containing Oxide Nanoparticles, *Journal of Heat Transfer*, *121*(2), 280–289.

[15] **Wang Xinwei**, **Xu Xianfan and S. Choi Stephen U.** (1999). Thermal Conductivity of Nanoparticle - Fluid Mixture, *Journal of Thermophysics and Heat Transfer*, *13*(4), 474–480.

[16] **Eastman, J.A.**, **Choi, S.U.S.**, **Li, S.**, **Yu, W. and Thompson, L.J.** (2001). Anomalously increased effective thermal conductivities of ethylene glycol-based nanofluids containing copper nanoparticles, *Applied Physics Letters*, *78*(6), 718–720.

[17] **Chopkar, M.**, **Sudarshan, S.**, **Das, P. and Manna, I.** (2008). Effect of Particle Size on Thermal Conductivity of Nanofluid, *Metallurgical and Materials Transactions A*, *39*(7), 1535–1542.

[18] **Putnam, S.A.**, **Cahill, D.G.**, **Braun, P.V.**, **Ge, Z. and Shimmin, R.G.** (2006). Thermal conductivity of nanoparticle suspensions, *Journal of Applied Physics*, *99*(8).

[19] **Zhang, X.**, **Gu, H. and Fujii, M.** (2006). Effective thermal conductivity and thermal diffusivity of nanofluids containing spherical and cylindrical nanoparticles, *Journal of Applied Physics*, *100*(4).

[20] **Buongiorno, J.**, **Venerus, D.C.**, **Prabhat, N.**, **McKrell, T.**, **Townsend, J.**, **Christianson, R.**, **Tolmachev, Y.V.**, **Keblinski, P.**, **Hu, L.w.**, **Alvarado, J.L.**, **Bang, I.C.**, **Bishnoi, S.W.**, **Bonetti, M.**, **Botz, F.**, **Cecere, A.**, **Chang, Y.**, **Chen, G.**, **Chen, H.**, **Chung, S.J.**, **Chyu, M.K.**, **Das, S.K.**, **Paola, R.D.**, **Ding, Y.**, **Dubois, F.**, **Dzido, G.**, **Eapen, J.**, **Escher, W.**, **Funfschilling, D.**, **Galand, Q.**, **Gao, J.**, **Gharagozloo, P.E.**, **Goodson, K.E.**, **Gutierrez, J.G.**, **Hong, H.**, **Horton, M.**, **Hwang, K.S.**, **Iorio, C.S.**, **Jang, S.P.**, **Jarzebski, A.B.**, **Jiang, Y.**, **Jin, L.**, **Kabelac, S.**, **Kamath, A.**, **Kedzierski, M.A.**, **Kieng, L.G.**, **Kim, C.**, **Kim, J.H.**, **Kim, S.**, **Lee, S.H.**, **Leong, K.C.**, **Manna, I.**, **Michel, B.**, **Ni, R.**, **Patel, H.E.**, **Philip, J.**, **Poulikakos, D.**, **Reynaud, C.**, **Savino, R.**, **Singh, P.K.**, **Song, P.**, **Sundararajan, T.**, **Timofeeva, E.**, **Tritcak, T.**, **Turanov, A.N.**, **Vaerenbergh, S.V.**, **Wen, D.**, **Witharana, S.**, **Yang, C.**, **Yeh, W.H.**, **Zhao, X.Z. and Zhou, S.Q.** (2009). A benchmark study on the thermal conductivity of nanofluids, *Journal of Applied Physics*, *106*(9).

[21] **Sarkar, S. and Selvam, R.P.** (2007). Molecular dynamics simulation of effective thermal conductivity and study of enhanced thermal transport mechanism in nanofluids, *Journal of Applied Physics*, *102*(7).

[22] **Li, L.**, **Zhang, Y.**, **Ma, H. and Yang, M.** (2008). An investigation of molecular layering at the liquid-solid interface in nanofluids by molecular dynamics simulation, *Physics Letters A*, *372*(25), 4541–4544.

[23] **Sankar, N.**, **Mathew, N. and Sobhan, C.** (2008). Molecular dynamics modeling of thermal conductivity enhancement in metal nanoparticle suspensions, *International Communications in Heat and Mass Transfer*, *35*(7), 867–872.

[24] **Ghosh, M.M.**, **Roy, S.**, **Pabi, S.K. and Ghosh, S.** (2011). A Molecular Dynamics-Stochastic Model for Thermal Conductivity of Nanofluids and Its Experimental Validation, *Journal of Nanoscience and Nanotechnology*, *11*(3), 2196–2207.

[25] **Xue, L.**, **Keblinski, P.**, **Phillpot, S.R.**, **Choi and Eastman, J.A.** (2004). Effect of liquid layering at the liquid-solid interface on thermal transport, *International Journal of Heat and Mass Transfer*, *47*(19-20), 4277–4284.

[26] **Keblinski, P.**, **Prasher, R. and Eapen, J.** (2008). Thermal conductance of nanofluids: is the controversy over?, *Journal of Nanoparticle Research*, *10*(7), 1089–1097.

[27] **Babaei, H.**, **Keblinski, P. and Khodadadi, J.M.** (2012). Equilibrium molecular dynamics determination of thermal conductivity for multi-component systems, *Journal of Applied Physics*, *112*(5).

[28] **Haile, J.M.** (1992). *Molecular Dynamics Simulation: Elementary Methods*, John Wiley & Sons, Inc., New York, NY, USA, 1st edition.

[29] **Hirschfelder, J.**, **Bird, R.B. and Curtiss, C.F.** (1964). *Molecular theory of gases and liquids; rev. version*, Structure of matter series, Wiley, New York, NY.

[30] **Fernández, G.**, **Vrabec, J. and Hasse, H.** (2004). A molecular simulation study of shear and bulk viscosity and thermal conductivity of simple real fluids, *Fluid Phase Equilibria*, *221*(1–2), 157–163.

[31] **Rapaport, D.C.** (2004). *The Art of Molecular Dynamics Simulation*, Cambridge University Press, New York, NY, USA, 2nd edition.

[32] **Evans, D.J. and Morriss, G.P.**, (1990). 6 - Computer Simulation Algorithms, **D.J. Evans and G.P. Morriss**, editors, Statistical Mechanics of Nonequilibrium Liquids, Academic Press, pp.121–168.

[33] **Allen, M.P. and Tildesley, D.J.** (1989). *Computer Simulation of Liquids*, Clarendon Press, New York, NY, USA.

[34] **Viscardy, S.**, **Servantie, J. and Gaspard, P.** (2007). Transport and Helfand moments in the Lennard Jones fluid. I. Shear viscosity, *The Journal of Chemical Physics*, *126*(18).

[35] **Viscardy, S.**, **Servantie, J. and Gaspard, P.** (2007). Transport and Helfand moments in the Lennard-Jones fluid. II. Thermal conductivity, *The Journal of Chemical Physics*, *126*(18).

[36] **Griebel, M.**, **Knapek, S. and Zumbusch, G.** (2007). *Numerical Simulation in Molecular Dynamics: Numerics, Algorithms, Parallelization, Applications*, Springer Publishing Company, Incorporated, 1st edition.

[37] **Kubo, R. and Ichimura, H.** (1990). *Statistical Mechanics: An Advanced Course with Problems and Solutions*, North-Holland personal library, North-Holland.

[38] **Grest, G.S. and Kremer, K.** (1986). Molecular dynamics simulation for polymers in the presence of a heat bath, *Phys. Rev. A*, *33*, 3628–3631.

[39] **Frenkel, D. and Smit, B.** (2001). *Understanding Molecular Simulation*, Academic Press, Inc., Orlando, FL, USA, 2nd edition.

[40] **Smit, B.** (1992). Phase diagrams of Lennard Jones fluids, *The Journal of Chemical Physics*, *96*(11), 8639–8640.

CURRICULUM VITAE

Name Surname: İrem Topal

Place and Date of Birth: İstanbul, 24 Jan 1990

E-Mail: topali@itu.edu.tr

EDUCATION:

- **B.Sc.:** 2014, İstanbul Technical University, Faculty of Sciences and Letters, Department of Physics Engineering
- **M.Sc.:** 2017, İstanbul Technical University, Graduate School of Sciences Engineering and Technology, Department of Physics Engineering

PROFESSIONAL EXPERIENCE AND REWARDS:

- 2013, Completed internship at the Department of Engineering at Eczacıbaşı-Monrol Nuclear Products.
- 2013, Received *Nuclear Medicine Physics Certification* from the Department of Nuclear Medicine of Cerrahpaşa Faculty of Medicine.